Assessment of Almond Water Status Using Inexpensive Thermographic Imagery

Project No.: **HORT31.Bailey**

Project Leader:
First/Last Name: Brian Bailey
Location: U.C. Davis
Mailing Address: One Shields Ave., Mail Stop #2, Davis, CA 95616
Phone: 530-752-7478
E-mail: bnbailey@ucdavis.edu

Project Cooperators and Personnel:
Cooperating Personnel:
- Bruce Lampinen, Department of Plant Sciences, U.C. Davis, bdlampinen@ucdavis.edu
- Astrid Volder, Department of Plant Sciences, U.C. Davis, avolder@ucdavis.edu

Personnel:
- Magalie Poirier-Pocovi, Post-doctoral scholar, Department of Plant Sciences, U.C. Davis, mdpoirier@ucdavis.edu

A. Summary

The overarching aim of this study is to develop a quick and inexpensive tool that can be used to evaluate almond tree water needs in order to help guide efficient irrigation practices. The tool is based on the use of inexpensive smartphone-based thermal cameras to measure leaf temperatures, which are used to infer leaf/canopy water status. Water lost by the leaf (transpiration) creates a cooling effect, and can reduce the leaf temperature to several degrees below the ambient air temperature in the case of a well-watered tree. As trees run out of water, transpiration begins to decline and the discrepancy between leaf and air temperature is reduced. However, transpiration is only one of several factors that affects the temperature of a leaf. A challenge is the separation of the effects of weather and environment from transpiration within the leaf temperature measurement, since ambient weather conditions also play an important role in determining the temperature of a leaf. This separation is typically performed using a crop water stress index or CWSI, which is purported to isolate the effects of plant water status within leaf/canopy temperature measurements.

We used a sensitivity analysis to show that the CWSI is as sensitive to wind speed as it is to plant water status, which can potentially introduce significant noise in the CWSI. This means that the CWSI must decline substantially before one can conclude that the tree has become “stressed”, because the decline in the CWSI itself must be much larger than the error in the CWSI measurement. We found this to be problematic in almond, potentially rendering the CWSI useless in certain cases. Our experiments showed that during the period of low to moderate stress, the CWSI was relatively insensitive. Trees needed to be very stressed (e.g., 1-2 weeks without water) in order to observe a statistically significant decline in CWSI. We tried calculating the CWSI based on individual leaf temperature in the sun/shade, whole-canopy temperature, and only the upper sunlit portion of the canopy, and found a similar result in all cases. Initial results indicated that formulation of a modified CWSI based on the

temperature of the trunk surface could potentially yield a water status indicator that was sensitive almost immediately following an irrigation event.

B. Objectives

1. Goal(s) and specific objectives of the proposal

The main aim of this study is to develop a smartphone application based on low-cost thermography that can be used to quickly evaluate tree water status and help guide irrigation decisions.

The research questions are:
Question 1. How does variation in environmental conditions (PAR, air temperature, relative humidity and wind speed) influence the crop water stress indices (CWSIs)?
Question 2. Can inexpensive thermography track the evolution of the water status decline of almond trees at various organ scales (leaf, canopy, or trunk) during a dry-down period?
Question 3. Can inexpensive thermography be used as a tool to schedule irrigation?

2. Annual outputs or milestones for each of the objectives

Table 1. Main Goal(s), key objectives, timelines and milestones

Main Goal: **Evaluate whether low-cost infrared thermography can be used as a tool for almond irrigation scheduling**		
Objective(s)	**Date to be accomplished**	**Milestones and deliverables associated to the objective**
Obj. 1 Develop a model for evapotranspiration (or other plant variables in connection with tree water status) inversion from thermographic imagery	July 2019	This objective is complete, and resulted in the submission of two scientific publications (one has been accepted).
Obj. 2a Collect field data for methodological development and testing	September 2020	This objective will produce experimental data for development and testing, and will be complete after all intensive observation periods have concluded. We have completed two field seasons of data collection, and will complete one more in 2020.
Obj. 2b Analyze field data for calibration and validation	December 2020	Analysis of data from years 1 and 2 has been used to quantify the performance of the method. A scientific publication is in prep., and will be submitted early 2020. Additional analysis will continue following the 2020 field season.
Obj. 3. Develop a smartphone application ("app") for distribution	N/A	Results to date suggest that thermography is not useful for irrigation scheduling in almond, and thus it will not be useful to develop an app.

C. Annual Results and Discussion

Obj. 1 - Impact of the environmental conditions and stomatal conductance on crop water stress indices (CWSI)

The goal of this part of the project was to better understand the impact of environmental conditions (PAR, air temperature, relative humidity and wind speed) and stomatal conductance on the CWSI. Ideally, we would like the CWSI to have low sensitivity to environmental factors, and high sensitivity to plant water status as indicated by the stomatal conductance. In order to quantify this sensitivity, a Morris sensitivity analysis was used to evaluate the impact of each parameter (environmental factors and stomatal conductance) on the CWSI value. We used the energy balance model to simulate the leaf temperature, the wet and dry reference surface temperature (components of CWSI) to evaluate four different formulations of CWSIs.

The most commonly used CWSI, defined as $CWSI_2 = (T_{dry} - T_L) / (T_{dry} - T_{wet})$, showed the best ratio between the sensitivity of environmental factors and stomatal conductance. According to the results of the sensitivity analysis, $CWSI_2$ has the desirable trait that all environmental variables (except wind speed) appear to have a linear impact.

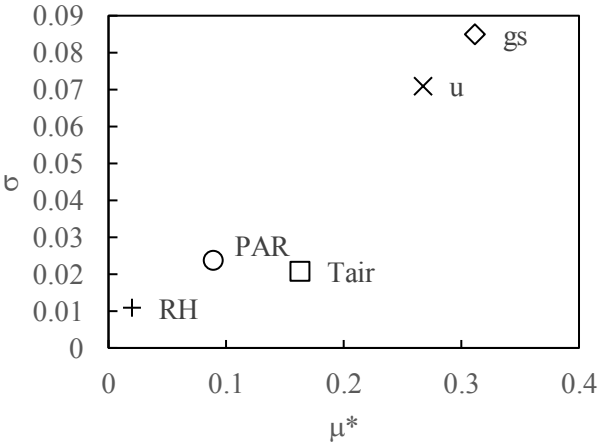

Figure 1 Example of global sensitivity analysis of CWSI (formulation 2) using the Morris method. Mean (μ* ranks the parameters according to the magnitude of their impacts on the CWSI) and standard deviation (σ indicates the non-linear and/or parameter interaction effects) of the elementary effects of air temperature (T_{air}), relative humidity (RH), photosynthetically active radiation (PAR), wind speed (u), and stomatal conductance (g_s) on $CWSI_2$ in the sun. [see Publication 1 for the details]

This CWSI is moderately sensitive to light and air temperature, and highly sensitive to wind speed and stomatal conductance (Figure 1). This means that significant variation in CWSI could be observed without any change in water status. This could create significant error, and may mean that plants must be very stressed before a statistically significant decline in CWSI is observed.

We also demonstrated that it is not recommended measure CWSIs in shaded conditions (leaf/canopy scales), but rather to perform measurements in full sun (i.e., PAR>700 μmol m^{-2} s^{-1}). The lack of strong radiative forcing increases the impact of other environmental variables such as T_{air} and decreases the impact of g_s.

The complete results are described in publication 1, attached at the end of this report.

Obj. 2 – Tracking the CWSI of well-irrigated and non-irrigated trees at various scales/organs (leaf, canopy, trunk)

Previous work has repeatedly shown that the CWSI approach is able to 'detect' differences between a well-watered crop and a water stressed crop. However, this does not tell us whether

the method can be used to schedule irrigation. A useful method should be able to detect the onset of stress soon after an irrigation event, and well before stomata have started to close in response to declining water potential.

We conducted a dry-down experiment in which the decline in tree water status was closely followed through time following a heavy irrigation event that ensured the soil profile was full. The experiment was conducted in Davis, CA, using four-year-old nonpareil trees grafted on Krymsk 86 rootstock. A number of instruments, including the thermographic camera, were used to measure the plant response to the dry-down and ultimately the onset of stress, which was defined as the point at which stomata first began to close when subjected to constant leaf environmental conditions.

The dry-down was observed for two treatments, one in which no water was applied, and the other being 'well-watered'. The midday water potential of the well-watered trees fluctuated around -0.9 MPa, which was slightly below the theoretical non-water stressed baseline (Figure 2a, red curve). The water status of the stressed trees gradually decreased from ca. -0.8 MPa to ca. -2.2 MPa during the non-irrigation period and was high (ca. -2.2 MPa) at the end of the measurement period (Figure 2a).

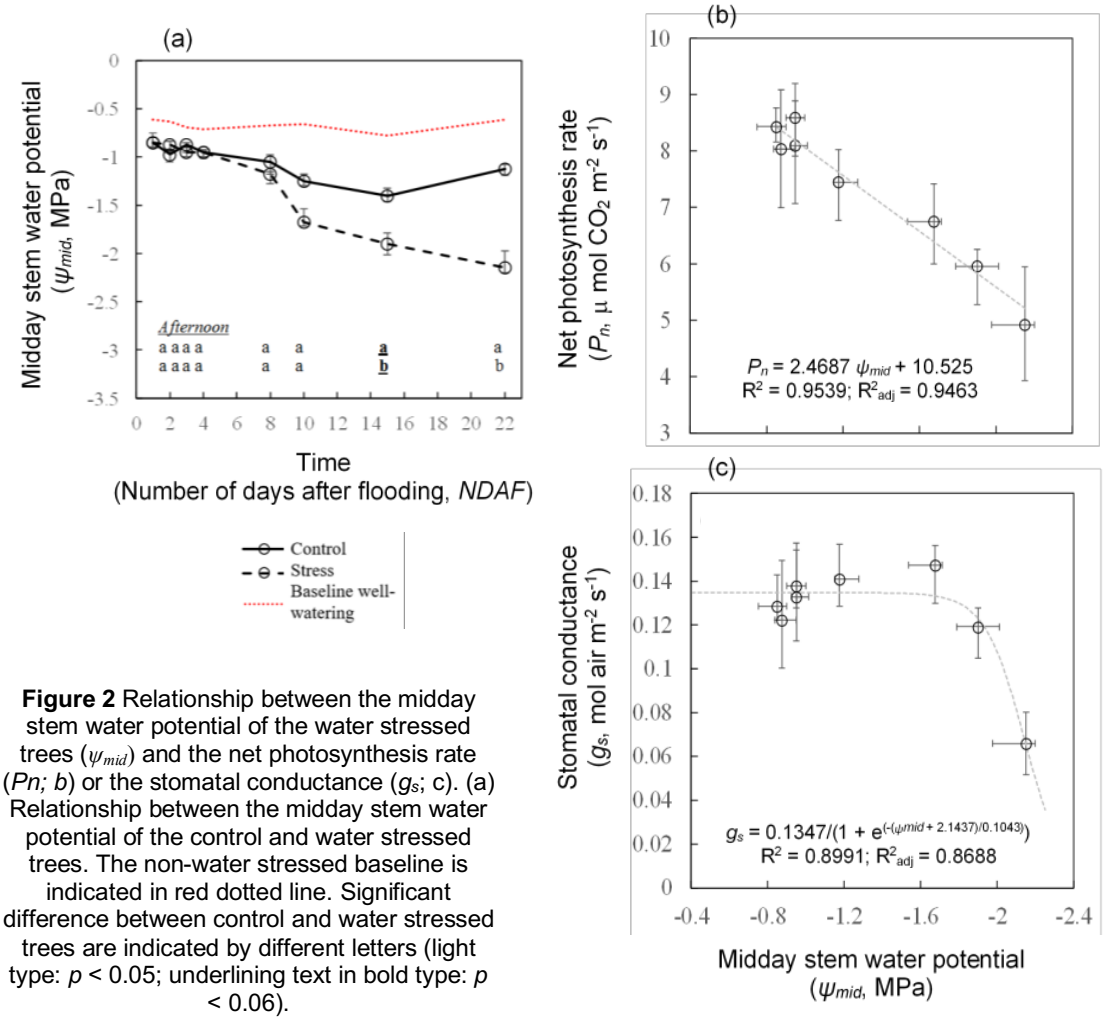

Figure 2 Relationship between the midday stem water potential of the water stressed trees (ψ_{mid}) and the net photosynthesis rate (*Pn; b*) or the stomatal conductance (g_s; c). (a) Relationship between the midday stem water potential of the control and water stressed trees. The non-water stressed baseline is indicated in red dotted line. Significant difference between control and water stressed trees are indicated by different letters (light type: $p < 0.05$; underlining text in bold type: $p < 0.06$).

The stomatal conductance decreased after the midday water potential fell below approximately ψ_{mid} = -1.7 MPa (Figure 2c), indicating the onset of stomatal closure. Decline in photosynthesis rate occurred sooner at ψ_{mid} values below ca. -1.2 MPa (Figure 2b). When the stomata began to close, the net photosynthesis rate had fallen to about 20% of its maximum rate.

While measurements of stem water potential and stomatal conductance indicated a clear onset of water stress midway through the experiment, the CWSI based on thermal imagery showed very little variation at both the leaf and canopy scales (Figure 3). CWSIs measured at the leaf scale had high variability, and only toward the end of the experiment was there a statistically significant difference between the well-watered and drought stressed treatments. CWSIs calculated based on whole-canopy or upper-canopy measurements were much more consistent with lower variability. However, there was still little difference between the well-watered and water stressed treatments until the end of the experiment.

Based on the data we have collected, the CWSI based on leaf, whole canopy, and upper canopy temperature, we could not distinguish a significant difference between the 'stress' and 'well-watered' treatments until stress was substantial (long after stomata have started to close; Figure 3a, b, c). This means that by the time the method can reliably detect the onset of stress, it is probably too late and yield may be affected.

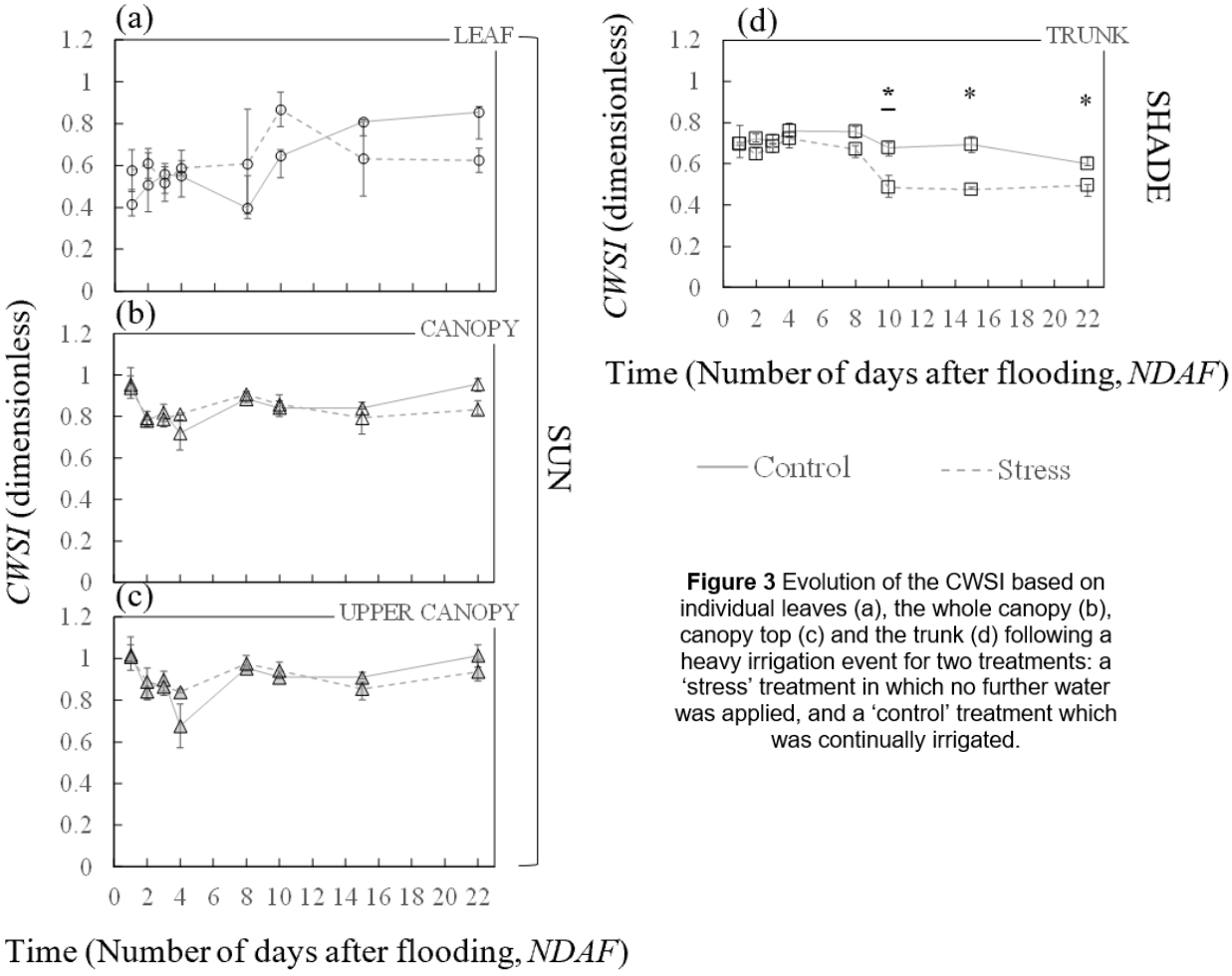

Figure 3 Evolution of the CWSI based on individual leaves (a), the whole canopy (b), canopy top (c) and the trunk (d) following a heavy irrigation event for two treatments: a 'stress' treatment in which no further water was applied, and a 'control' treatment which was continually irrigated.

We did find evidence suggesting a CWSI based on trunk temperature could be a sensitive indicator of plant water status starting soon after the dry-down began (Figure 3d). These results need to be further verified with additional experiments.

Conclusion

To conclude, in many cases, thermography may be able to detect areas of the orchard with significant variation in plant water status at any single instant in time. However, we have not yet found evidence to suggest that thermography along with the traditional leaf/canopy CWSI is a potentially viable tool for scheduling irrigation because of the lack of sensitivity of the CWSI throughout time as water status declines following an irrigation event. Our results indicated that the traditional CWSI is moderately sensitive to light and air temperature, and highly sensitive to wind speed. This may contribute to lack of sensitivity of the CWSI during the initial period when stomata begin to close.

Future work could further improve calculation of CWSIs by developing a normalization that can remove the impact of the wind speed. It is also necessary to verify results for other almond cultivars and soil textures. Finally, additional experiments are needed to explore the calculation of the CWSI based on trunk temperature (i.e., improve the formulation of the stress index).

D. Outreach Activities

1. Outreach activities including the event description

- Almond Board Conference in 2017, 2018, and 2019.
- Invited Talk: "Development of the Next Generation of Perennial Crop Modeling Tools", CalASA/California Plant and Soil Conference, Fresno, CA.

E. Materials and Methods *(500 word max.)*:

1. Outline materials used and methods to conduct experiment(s)

Plant material

During the 2019 growing season, we worked on the same almond orchard as the 2018 growing season. We used the *Prunus dulcis* cultivar “Non Pareil” grafted on Krymsk 86 rootstock.

Figure 4 Experimental almond orchard used in the study (in collaboration with Dr. Astrid Volder, U.C. Davis).

Experimental procedure
The following group of measurements were simultaneously collected:
• Organ surface temperature: Thermal images were obtained for leaves and whole trees with a FLIR smartphone camera (FLIROne® Pro for iOS) connected to an iPhone. This provided the spatial distribution of surface temperature across the leaf, the canopy or the trunk, and forms the basis of the measurement technique.
The dry and wet reference surfaces temperature (T_{dry} and T_{wet}) for the leaf and the canopy are defined from the temperature of a green paper (T_{ref}) and by using 2 linear models (one for T_{dry} and one for T_{wet}; publication 2 p. 32). For the trunk, T_{dry} was defined by T_{air} + 7°C and T_{wet} by $T_{soil\ at\ 15cm}$ − 7°C (based on the second law of the thermodynamic and the water flux circulating in the trunk).
• Water potential (ψ): Immediately after the taking pictures, the water potentials of the leaf were measured using a pressure chamber.
• Meteorological data: The air temperature (T_{air}), the relative humidity (*RH*) and the soil temperature at 15 cm ($T_{soil\ at\ 15cm}$) were obtained from either the weather station of the CIMIS network or locally near the studied trees with a thero-hygrometer probe for smartphone (T_{air} and *RH*).
• Current stomatal conductance, net photosynthesis rate: Gas exchange measurements with saturating light (current stomatal conductance and net photosynthesis rate) were carried out using an LI-6800 portable photosynthesis system for the leaf.

F. Publications that emerged from this work

1. List peer review publications in preparation, accepted or published

Accepted publications:

- **Poirier-Pocovi, M., Bailey, B.N. 2020.** Sensitivity analysis of four crop water stress indices to ambient environmental conditions and stomatal conductance. *Scientia Horticulturae*. 259, *in press*. https://doi.org/10.1016/j.scienta.2019.108825 (see p. 8)

Submitted publications:

- **Poirier-Pocovi, M., Volder, A., Bailey, B.N. 2020.** Modeling of reference temperatures for calculating crop water stress indices from infrared thermography. *Agricultural Water Management*. Moderate modifications. *Submitted process in progress* (see p. 32)

Publications in preparation:

- **Poirier-Pocovi, M., Bailey, B.N. 20xx.** Tracking the tree water status of *Prunus dulcis* with thermal imaging (accessory for smartphone) to schedule the irrigation.

2. Other publications (e.g. outreach materials)

3 posters during the Almond Board conference in December 2017, 2018 and 2019:

- **Bailey, B.N. 2017.** Assessment of Almond Water Status using Inexpensive Thermal Imagery. Almond Board Conference 2017. Sacramento, California (USA), 5-7 December 2018.
- **Poirier-Pocovi, M., Bailey, B.N. 2018.** Assessment of Almond Water Status using Inexpensive Thermal Imagery. Almond Board Conference 2018. Sacramento, California (USA), 4-6 December 2018.

- **Poirier-Pocovi, M., Bailey, B.N. 2019.** Assessment of Almond Water Status using Inexpensive Thermal Imagery. Almond Board Conference 2018. Sacramento, California (USA), 10-12 December 2018.

3. Copies of publications

Only the accepted and submitted publications are provided with this annual report.

Publication 1

ORIGINAL ARTICLE

Sensitivity analysis of four crop water stress indices to ambient environmental conditions and stomatal conductance

Magalie Poirier-Pocovi[a], Brian N. Bailey*[a]

*For correspondence, E-mail: mdpoirier@ucdavis.edu

[a] University of California, Department of Plant Sciences, One Shields Avenue, Davis, California 95616-8571, U.S.A.

Highlights

- Sensitivity of CWSIs to ambient conditions and stomatal conductance was analyzed.
- Performance was assessed from sensitivity to stomata relative to ambient conditions
- All CWSIs were highly sensitive to wind speed
- All CWSIs performed poorly in shaded conditions
- Two CWSIs performed well in sunny conditions and removed most environmental effects

ABSTRACT

Crop water stress indices (CWSIs) quantify plant water status based on measurement of plant temperature. The goal of CWSI formulation is to normalize measured leaf temperatures based on reference temperatures to remove sensitivity to ambient environmental conditions (*e.g.*, air temperature, humidity, radiation), while retaining sensitivity to plant water status as reflected by stomatal conductance. This study sought to better understand the sensitivity of these temperatures to ambient environmental conditions, and ultimately how they influence various CWSIs. The surface energy balance was modeled to simulate the impacts of input parameter variation on leaf temperature and reference surface temperatures used to calculate four different CWSIs. The performance of the CWSIs were assessed based on their ability to maximize sensitivity to stomatal conductance while minimizing the relative sensitivity to ambient environmental conditions.

The sensitivity analyses indicated that all four CWSIs performed poorly in shaded conditions, as they had relatively low sensitivity to stomatal conductance and were sensitive to all environmental parameters. Two CWSIs had high sensitivity to stomatal conductance, and low sensitivity to all environmental parameters except wind speed. None of CWSIs could remove sensitivity to all environmental parameters while retaining sensitivity to stomatal conductance.

Keywords: Energy balance equation, crop water stress index, leaf temperature, sensitivity analysis, Morris method, OAT method

1. INTRODUCTION

Water availability is becoming the most limiting factor for crop production in most countries of the world. In many regions, changing precipitation or melting snow and ice are altering hydrological systems, affecting water resources in terms of quantity and quality (IPCC, 2014). Adaptive water management techniques (*i.e.*, adjusting the water supply according to the water needs of the crop to decrease water waste) can help adapt to uncertain hydrological conditions due to climate change.

Woody perennial fruit and nut crops generally require extensive and variable irrigation in order to maximize yields or manipulate quality (Patumi *et al.*, 1999; Goldhamer and Beede, 2004; Egea *et al.*, 2009; García-Tejero *et al.*, 2010), and thus there is a need for sensitive, robust, and user-friendly techniques for measurement of tree water status. To provide guidance for irrigation scheduling, crop water stress index (CWSI) approaches have been previously developed to relate leaf and canopy temperatures to plant water stress conditions (Idso, 1982; Jackson *et al.*, 1981; Grant *et al.*, 2007; García-Tejero *et al.*, 2018). The calculation of these indices helps to estimate the water stress of a plant by comparing its leaf or canopy temperature (T_L) with that of a non-water-stressed plant (T_{wet}) and a dry plant (T_{dry}) to formulate a normalized indicator of plant water status (Nanda *et al.*, 2018). Many CWSIs have been proposed that are based on some combination of wet and dry reference surface temperatures, each with the goal of increasing sensitivity of the index to water stress while decreasing sensitivity to environmental conditions (*e.g.*, Jackson *et al.*, 1981; Qiu *et al.*, 1996; Jones *et al.*, 1997, 2002; Jones, 1999; Grant *et al.*, 2007). These CWSIs are typically formulated arbitrarily or loosely based on theoretical arguments, and an objective theoretical evaluation of their performance has yet to be performed. Quantitative evaluation of CWSIs in the natural environment is difficult because controlling or separating the effects of each environmental factor is generally not possible, and measurement errors become compounded with the formulation of the CWSI itself.

In order to better understand how the different CWSIs are influenced by environmental variables, and ultimately the degree to which they are correlated with stomatal conductance, this study proposes to use a mathematical model based on the energy balance equation along with data obtained in an almond orchard to conduct a sensitivity analysis of different CWSIs and the associated temperature values on which they are based. The aims of this study were thus to (1) evaluate the sensitivity

of T_{dry}, T_{wet} and T_L to the variation of four important environmental factors (air temperature, relative humidity, absorbed photosynthetically active radiation, and wind speed) and stomatal conductance, (2) evaluate the sensitivity of four CWSIs following to these parameter variations, and (3) determine the best CWSI for inferring plant water status, which we considered, as to be the CWSI that has maximal sensitivity to stomatal conductance compared to its sensitivity to environmental conditions.

2. MATERIAL AND METHODS

2.1. Plant material

The range of the parameters in the sensitivity analysis was determined using an experimental dataset collected in a four-year-old almond orchard (*Prunus dulcis* Mill. cv. 'Non Pareil') at the University of California, Davis (altitude: 23 m, on average; 38°32'16"N, 121°47'42"W).

2.2. Sampling strategy

All measurements were collected in the morning between 9:00 am and 12:00 pm in August of 2018. 64 leaves with approximately the same orientation and size were chosen: in the shaded zone inside the canopy (1 leaf × [6 trees × 2 dates + 4 trees × 5 dates]; 10 < PAR < 300 μmol photons m^{-2} s^{-1}), and in the sunny zone outside the canopy (1 leaf × [6 trees × 2 dates + 4 trees × 5 dates]; 700 < PAR < 1750 μmol photons m^{-2} s^{-1}).

2.3. Stomatal conductance measurement

Gas exchange measurements were carried out using a LI-6800 portable photosynthesis system (LI-COR, Inc., Lincoln, NE, USA). One marked leaf was located in the shade and another marked leaf was situated under the sun. A portion of each leaf of interest was placed in a cuvette with a 1 × 3 cm aperture equipped with an LED light source (6800-02B, LI-COR, Inc.). The CO_2 concentration inside the cuvette was set at 400 μmol CO_2 mol^{-1}. The values of stomatal conductance (mol air m^{-2} s^{-1}) were recorded once there was stabilization of the measurement. The air temperature (T_{air}) and relative humidity (RH) inside the chamber, was set manually to match ambient conditions as measured by a handheld thermo-hygrometer probe for smartphones (model 800014, TFA® Dostmann GmbH & Co.KG, Wertheim, Germany). Similarly, the light inside the chamber was set to match the flux measured by the external quantum sensor of the LI-6800.

2.4. Description of the surface energy balance model (EBM)

Assuming that heat storage and metabolic heat production are negligible, the energy balance of a leaf is given by the following equation describing a balance between fluxes due to absorbed radiation, convection, and latent cooling (Campbell and Norman, 1998):

$$R_{abs} - \varepsilon_L \sigma T_L^4 - C_p g_H (T_L - T_{air}) - \lambda g_M \frac{e_s(T_L) - e_s(T_{air}) RH}{P_{atm}} = 0, \quad (1)$$

where R_{abs} (W m^{-2}) is the absorbed all-wave radiation flux (shortwave (*PAR* and near-infrared radiation) + longwave (emission from sky, ground and leaves)), ε_L is the leaf emissivity which was assumed to be equal to 0.96 (García-Tejero *et al.*, 2018), $\sigma = 5.67 \times 10^{-8}$ W m^{-2} K^{-4} is the Stefan-Boltzmann constant, T_L (K) is the temperature of the leaf, C_p = 29.3 J mol^{-1} K^{-1} is the specific heat of air, T_{air} (K) is the air temperature outside of the leaf boundary layer, λ = 44 000 J mol^{-1} is the latent heat of vaporization of water at 25 °C, $e_s(T_L)$ and $e_s(T_{air})$ (Pa) are respectively the saturation vapor pressures evaluated at the leaf or air temperature which were calculated using the Tetens equation (Campbell and Norman, 1998), *RH* is the relative humidity of air outside the leaf boundary layer, and P_{atm} (Pa) is the atmospheric pressure which was estimated as a function of elevation following Piedallu and Gégou, (2007). g_H (mol air m^{-2} s^{-1}) is the boundary layer conductance to heat and is calculated by the following equation, which is applicable for wind speed u < 2.5 m s^{-1} (Daudet *et al.*, 1999):

$$g_H = (10u + 7.1) \times \frac{12.265}{101300} \times \frac{P_{atm}}{T_{air}}. \quad (2)$$

g_M (mol air m^{-2} s^{-1}) is the leaf boundary-layer conductance to moisture and is defined by the following equation:

$$g_M = \frac{0.97\, g_H g_s}{(0.97 g_H) + g_s}, \quad (3)$$

where g_s is the stomatal conductance of the leaf (mol air m^{-2} s^{-1}). R_{abs} was estimated for a leaf fully exposed to the sky as

$$R_{abs} = R_{SW} + R_{LW} \approx \alpha \left(2 \times \frac{PAR}{4.6}\right) + \varepsilon_L \varepsilon_{air} \sigma T_{air}^4, \quad (4)$$

where R_{SW} and R_{LW} (W m^{-2}) are respectively the absorbed shortwave and the longwave radiation fluxes. α = 0.4 is the fraction of incident shortwave radiation that is absorbed by the leaf (absorptivity) (Susorova *et al.*, 2013), *PAR* is the absorbed photosynthetically active photon flux density (µmol m^{-2} s^{-1}; Sager and Mc Farlane, 1997), ε_{air} is the effective emissivity of the air, which was assumed to be ε_{air} = 0.5 (for clear sky; Sicart *et al.*, 2003). The factor of 4.6 converts *PAR* photon flux to energy

flux (Sager and Mc Farlane, 1997), and the factor of 2 approximates the conversion from energy flux in the *PAR* band to total shortwave energy flux.

For a leaf covered in liquid water, there is no stomatal limitation to transpiration and Eqn. 1 can be written as:

$$R_{abs} - \varepsilon_L \sigma T_{wet}^4 - C_p g_H (T_{wet} - T_{air}) - \lambda 0.97 g_H \frac{e_s(T_{wet}) - e_s(T_{air}) RH}{P_{atm}} = 0, \quad (5)$$

where T_{wet} is the temperature of the wet leaf.

For a non-transpiring leaf, the latent term is zero and Eqn. 1 can be written as:

$$R_{abs} - \varepsilon_L \sigma T_{dry}^4 - C_p g_H (T_{dry} - T_{air}) = 0, \quad (6)$$

where T_{dry} is the temperature of the non-transpiring leaf.

Because of the nonlinear nature of Eqns. 1, 5, and 6, they cannot be solved analytically for temperature. A numerical solution for T_L, T_{wet}, and T_{dry} was obtained using the "Solver" add-in for Microsoft Excel (Office 365 ProPlus for Windows) by varying the temperature value in order to achieve a net energy flux residual as close to zero as possible.

2.5. Crop Water Stress Indices

Several crop water stress indices (CWSIs) were evaluated in this study, which are based on some combination of T_L, T_{wet}, or T_{dry}. A first CWSI based only on T_{dry} and T_L was calculated as follows

$$CWSI_1 = \frac{T_{dry} - T_L}{T_{dry}}. \quad (7)$$

Since $T_{dry} \geq T_L$, $CWSI_1 \geq 0$, with $CWSI_1 = 0$ for a non-transpiring leaf, and $CWSI_1$ increasing as the crop becomes increasingly hydrated.

A second CWSI was calculated as follows (also called $CWSI_{NI/FI}$ by Grant *et al.*, 2007)

$$CWSI_2 = \frac{T_{dry} - T_L}{T_{dry} - T_{wet}}, \quad (8)$$

Since $T_L \geq T_{wet}$, $0 \leq CWSI_2 \leq 1$ in theory. However, unless liquid water is present on the exterior of the leaf under investigation (*e.g.*, rain, dew) or the vapor pressure deficit is zero, T_L will usually be significantly greater than T_{wet}, and thus $CWSI_2$ is unlikely to reach 1 in a fully-irrigated crop.

A third CWSI based only on T_{wet} and T_L was calculated as follows

$$CWSI_3 = \frac{T_L - T_{wet}}{T_{wet}}. \quad (9)$$

Using this approach, $CWSI_3 \geq 0$ in theory, with $CWSI_3$ increasing as the crop dries out.

Finally, a fourth CWSI derived by Jones (1999) is defined as follows

$$I_G = \frac{T_{dry} - T_L}{T_L - T_{wet}}. \quad (10)$$

A strength of this formulation is that it is theoretically proportional to stomatal conductance (Jones *et al.*, 2002), thus making its interpretation in a relative sense straightforward. However, it has the theoretical bounds of $0 \leq I_G \leq \infty$, and thus is not normalized to unity, which is because stomatal conductance is also not bounded.

2.6. Sensitivity analysis

A sensitivity analysis was used to quantify how the changes in environmental factors T_{air}, RH, PAR, and u (inputs) affected T_{dry}, T_{wet}, T_L and the four CWSIs (outputs), and ultimately to infer the expected performance of the CWSIs. For this analysis, a given combination of input parameters were used to determine the associated T_L, T_{wet}, T_{dry} values based on Eqns. 1, 5, and 6, which were then used to calculate each of the four CWSIs (Figure 1).

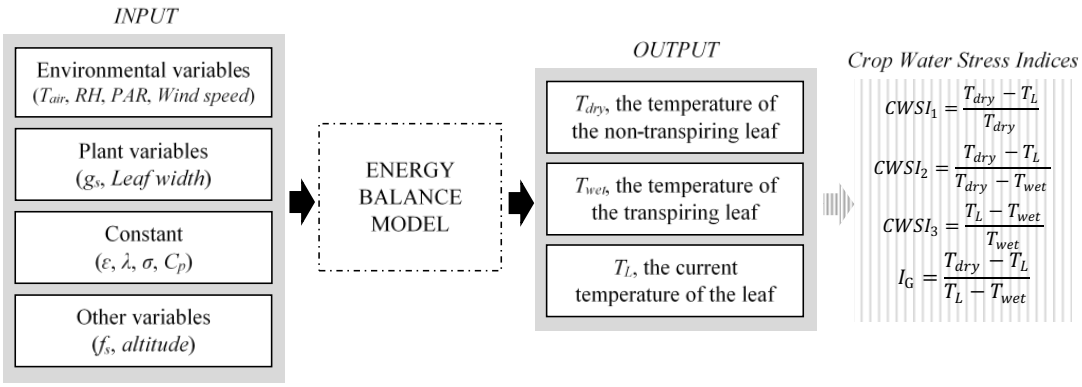

Fig.1: *Schematic representation of the inputs and outputs of the energy balance model and the crop water stress indices.*

The sensitivity analysis in this study utilized two well-known methods. The first was based on the one-factor-at-a-time method (OAT or OFAT method) to individually evaluate the impact of each input parameter on the output. The OAT method involves systematically varying one input variable while keeping others at their baseline (initial) values, and repeating for each of the other inputs in the same way.

A limitation of the OAT method is that it can be heavily dependent on the chosen parameter range and reference values, and that it does not incorporate interactions between input variables. This was addressed by also performing a "global" sensitivity analysis based on the Morris Method (Morris, 1991). The Morris Method randomly

samples input parameters to generate a distribution of "elementary effects" of the input parameters on the output. Sensitivity is quantified by calculating the mean of absolute values, μ^*, and standard deviation, σ, of the elementary effects distribution. The relative influence of each input parameter can be ranked based on the magnitude of μ^*, and the relative magnitude of σ with respect to the value of μ^* corresponds to non-linear and/or parameter interaction effects. The calculation of μ^* and σ was performed with the SAFE Toolbox for GNU Octave/MATLAB (Pianosi *et al*. 2015; Eaton *et al*., 2018), with the number of model evaluations chosen to be 2400.

The range of parameter values in the OAT and Morris method sensitivity analyses was based on measurements collected during the experimental campaign in August 2018, and are typical for the California region where almond trees are cultivated (Table 1). In the OAT method, the initial value of the parameters is the central value of the range (Table 1).

3. RESULTS

The values of T_{dry}, T_{wet}, T_L and the four CWSIs ($CWSI_1$, $CWSI_2$, $CWSI_3$ and I_G) at the initial parameter values (Table 1) are equal to 27.1 ^oC, 20.6 ^oC, 24.3 ^oC, 0.11, 0.44, 0.18 and 0.78 (respectively) in the sun. In the shade, these values decrease and are equal to 20.0 ^oC, 17.8 ^oC, 19.3 ^oC, 0.03, 0.29, 0.09 and 0.41 (respectively).

3.1. Sensitivity analysis of T_{dry}, T_{wet}, T_L and the four CWSIs to the variation of T_{air} based on the OAT method

Figure 2 shows the simulated effect of the individual variation of T_{air} between 15 ^oC and 40 ^oC on the models' outputs T_{dry}, T_{wet}, T_L and the four CWSIs in the sun and in the shade. T_{air} had a positive effect on T_{dry}, T_{wet}, T_L, $CWSI_2$ and I_G, and a negative effect on $CWSI_1$ and $CWSI_3$. The sensitivity of T_{dry}, T_{wet}, and T_L to variation in T_{air} were similar. In the sun (Fig. 2a), the variation of T_{dry}, T_{wet} and T_L was as large as ± 40% over the chosen range of T_{air} (15-40 ^oC). In the shade (Fig. 2b), the temperature variation due to T_{air} was up to ± 60%. $CWSI_1$ was the least sensitive and I_G was the most sensitive to the variation of T_{air} in both the sun (Fig. 2c) and in the shade (Fig. 2d). Furthermore, the simulation showed that the sensitivity of $CWSI_1$, $CWSI_2$ and $CWSI_3$ to the variation of T_{air} was essentially the same in the sun and shade. I_G was more sensitive to the variation of T_{air} in the sun than in the shade (Fig. 2c, 2d).

Table 1: *Parameter ranges and constant values used in the sensitivity analyses.*

	Parameter/ Variable	Definition	Units	Bounds	Initial value
Subject to SA	T_{air}	Air temperature	^{o}C	[15 - 40]	27.5
	RH	Relative humidity	%	[30 - 70]	50
	PAR	Photosynthetically active radiation	µmol photons m^{-2} s^{-1}	Sun: [700 - 1750] Shade: [10 - 300]	Sun: 1225 Shade: 155
	u	Wind speed	m s^{-1}	[0 - 2]	1
	g_s	Stomatal conductance	mol H_2O m^{-2} s^{-1}	Sun: [0.07 – 0.3] Shade: [0.02 – 0.2]	Sun: 0.185 Shade: 0.11
Not subject to SA	*l*	Width of the leaf	cm	2	
	ε_L	Emissivity of the leaf	dimensionless	0.96	
	ε_{air}	Emissivity of the air	dimensionless	0.5	
	α	Absorptivity	dimensionless	0.4	
	σ	Stefan-Boltzmann constant	W m^{-2} K^{-4}	5.67×10^{-8}	
	λ	Latent heat of vaporization at 25 ^{o}C	J mol^{-1}	44000	
	C_p	Specific heat of the air	J mol^{-1} K^{-1}	29.3	
	f_s	Relative humidity of the air immediately above the surface evaporating site	%	100	
	z	Altitude	m	22	

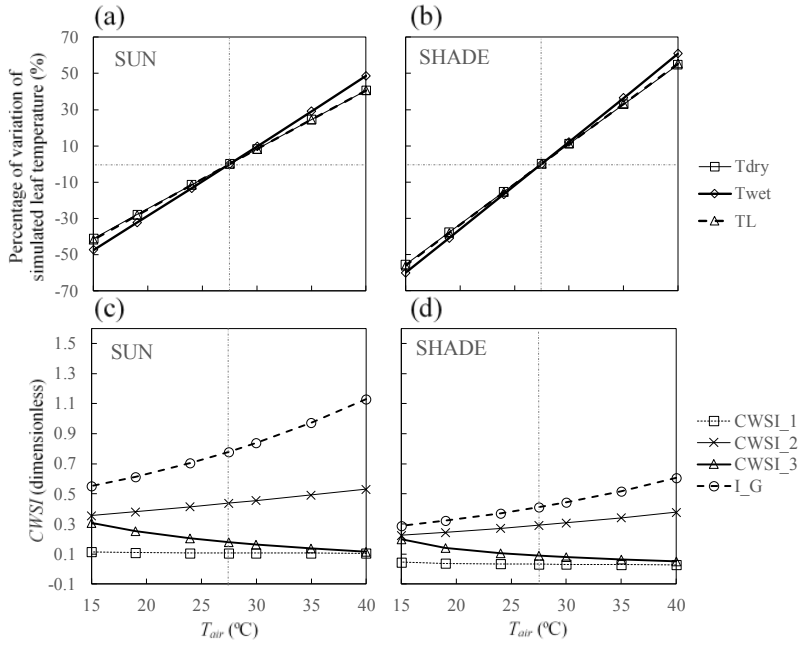

Fig.2: *OAT sensitivity analysis of air temperature. Percentage of variation of the simulated values of T_{dry}, T_{wet}, and T_L (a, b) and four CWSIs (c, d) due to variation in air temperature T_{air} in the sun (a, c) and shade (b, d).*

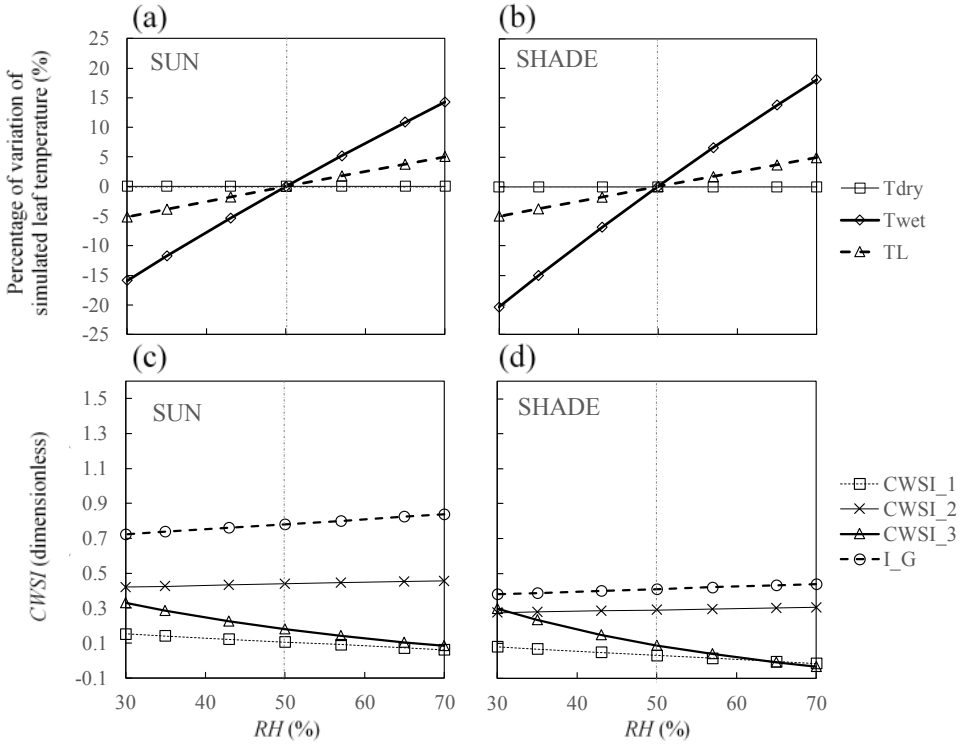

Fig.3: *OAT sensitivity analysis of relative humidity. Percentage of variation of the simulated values of T_{dry}, T_{wet}, and T_L (a, b) and four CWSIs (c, d) due to variation in relative humidity RH in the sun (a, c) and shade (b, d).*

3.2. Sensitivity analysis of T_{dry}, T_{wet}, T_L and the four CWSIs to the variation of RH based on the OAT method

Figure 3 shows the simulated effect of the variation of *RH* between 30 % and 70 % on the models' outputs T_{dry}, T_{wet}, T_L and the four CWSIs in the sun and in the shade. *RH* had a positive effect on T_{wet}, T_L, $CWSI_2$ and I_G and a negative effect on $CWSI_1$ and $CWSI_3$. T_{dry} is not sensitive to the variation of the relative humidity at constant T_{air} because there is no evaporation (Eqn. 6). The sensitivity of T_L to the variation of *RH* was up to ± 5% and was the same in the sun and shade (Fig. 3a, 3b). T_{wet} was the most sensitive output to the variation of *RH* and the effect was higher in the shade than in the sun. In the sun, the variation of T_{wet} to the variation of *RH* was up to ± 15%. In the shade, it could reach up to about ± 20%. The CWSIs showed the same variations in the sun and in the shade over the range of *RH* considered.

3.3. Sensitivity analysis of T_{dry}, T_{wet}, T_L and the four CWSIs to the variation of PAR based on the OAT method

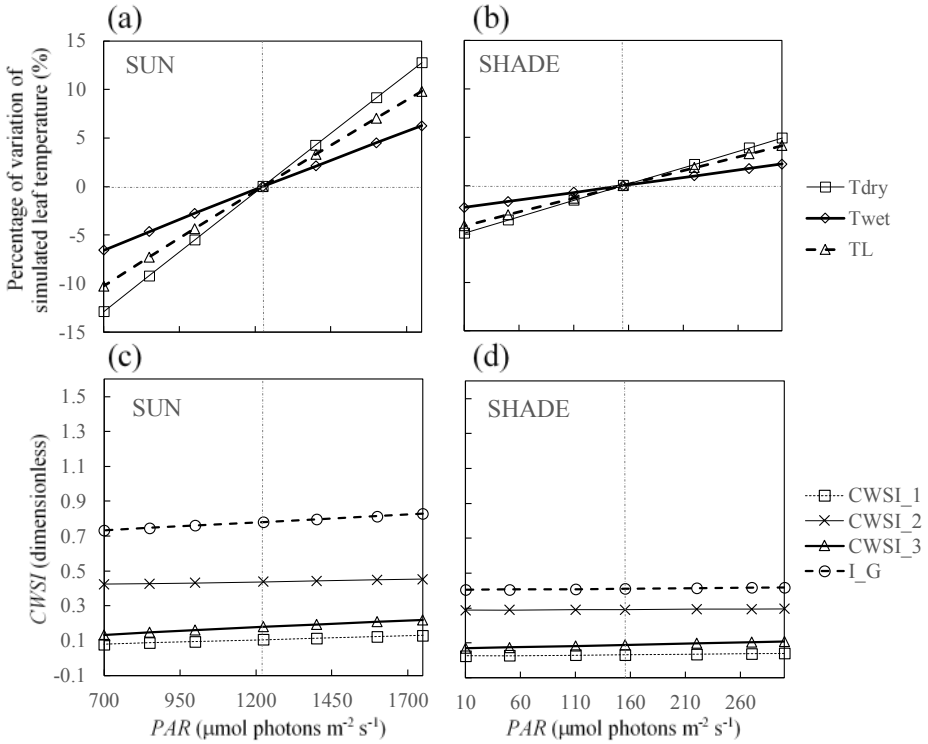

Fig.4: *OAT sensitivity analysis of radiation. Percentage of variation of the simulated values of T_{dry}, T_{wet}, and T_L (a, b) and four CWSIs (c, d) due to variation in photosynthetically active radiation PAR in the sun (a, c) and shade (b, d).*

Figure 4 shows the simulated effect of the variation of *PAR* between 700 and 1750 µmol photons m^{-2} s^{-1} in the sun and between 10 and 300 µmol photons m^{-2} s^{-1} in the shade on the outputs T_{dry}, T_{wet}, T_L and the four CWSIs. *PAR* had a positive effect on all models' outputs. The change in T_{wet}, T_L and T_{dry} over the chosen range of *PAR* were about ± 7 %, ± 10% and ± 13 % in the sun (Fig. 4a). The changes decreased in the shade to about ± 4% for T_{dry} and T_L and about ± 2% for T_{wet} (Fig. 4b). The sensitivities of the four CWSIs to *PAR* were relatively low (variation up to about ± 0.05) in the sun (Fig. 4c) and in the shade (Fig. 4d).

3.4. Sensitivity analysis of T_{dry}, T_{wet}, T_L and the four CWSIs to the variation of u based on the OAT method

Figure 5 shows the simulated effect of the variation of *u* between 0 and 2 m s^{-1} in the sun and in the shade on the models' outputs T_{dry}, T_{wet}, T_L and the four CWSIs.

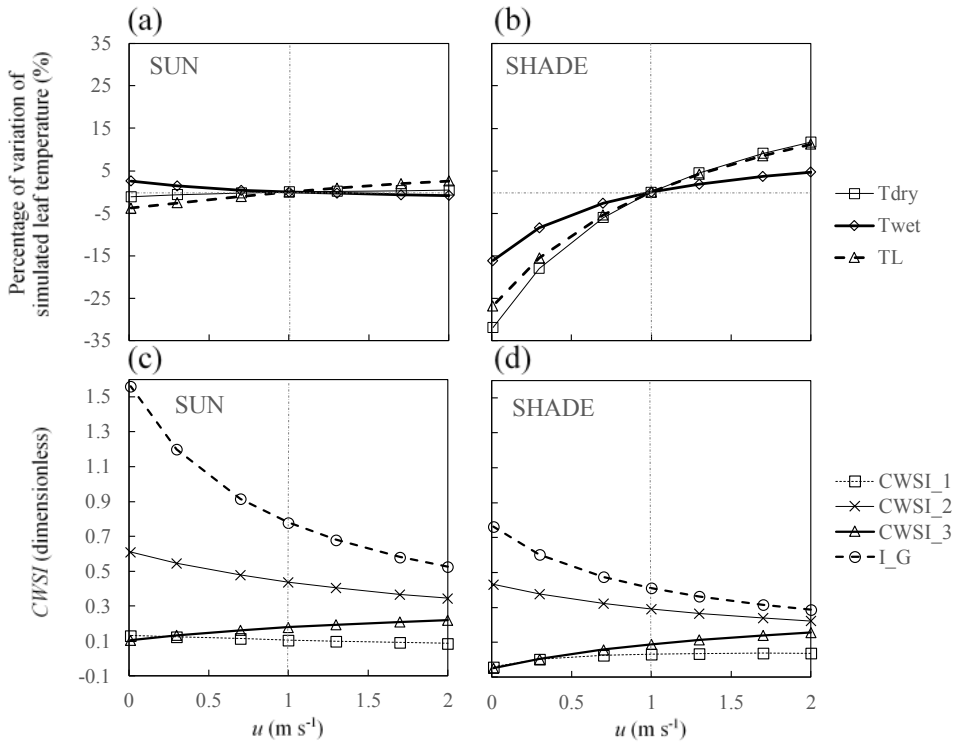

Fig.5: *OAT sensitivity analysis of wind speed. Percentage of variation of the simulated values of T_{dry}, T_{wet}, and T_L (a, b) and four CWSIs (c, d) in the sun (a, c) and shade (b, d) due to variation in wind speed u.*

In the sun, *u* had a positive effect on T_{dry}, T_L and $CWSI_3$ and a negative effect on T_{wet}, $CWSI_1$, $CWSI_2$ and I_G (Fig. 5a, 5c). In the shade, *u* had a positive effect on T_{dry}, T_{wet}, T_L, $CWSI_3$, $CWSI_1$ and a negative effect on $CWSI_2$ and I_G (Fig. 5b, 5d). In the sun, the

leaf temperatures were less influenced by the wind speed than in the shade (variation of the leaf temperatures < ± 5 %; Fig. 5a, 5b). In contrast, in the shade (Fig. 5b), for u > 1 m s^{-1}, the sensitivity of T_{wet} to the variation of u reached up to 5% and about 10 % for T_{dry} and T_L. For u < 1 m s^{-1}, the sensitivity of T_{wet} to the variation of u reached as much as -15% and about -30 % for T_{dry} and T_L. $CWSI_1$ and $CWSI_3$ showed a low sensitivity to the variation of u between 0 and 2 m s^{-1} in the sun and shade. In contrast, I_G had a high sensitivity to the variation of u in the sun, which was higher for the values of u < 1 m s^{-1} (Fig. 5c). In the shade, I_G had a reduced sensitivity to the variation of u compared to sunny conditions (Fig. 5d). $CWSI_2$ had moderate sensitivity to u in both the sun and shade, with sensitivity decreasing in the shade.

3.5. Sensitivity analysis of T_{dry}, T_{wet}, T_L and the four CWSIs to the variation of g_s based on the OAT method

Figure 6 shows the simulated effect of the individual variation of g_s between 0.07 and 0.3 mol m^{-2} s^{-1} in the sun and between 0.02 and 0.2 mol m^{-2} s^{-1} in the shade on the models' outputs T_{dry}, T_{wet}, T_L and the four CWSIs.

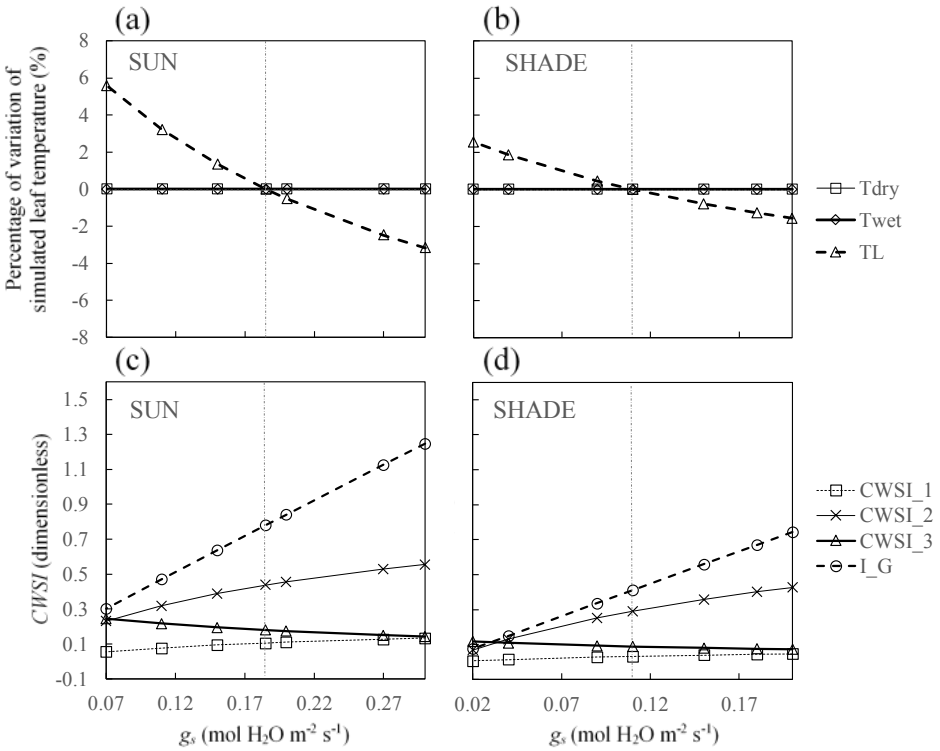

Fig.6: *OAT sensitivity analysis of stomatal conductance. Percentage of variation of the simulated values of T_{dry}, T_{wet}, and T_L (a, b) and four CWSIs (c, d) due to variation in stomatal conductance g_s in the sun (a, c) and shade (b, d).*

g_s does not influence T_{dry} and T_{wet} (see Eqn. 1, 5 and 6). The effect on T_L is negative and is more important in the sun than in the shade (Fig. 6a, 6b). For the CWSIs, g_s has a positive effect on $CWSI_1$, $CWSI_2$, I_G and a negative effect on $CWSI_3$. The sensitivities of $CWSI_1$ and $CWSI_3$ to the variation of g_s were very low, relatively low for $CWSI_2$, and high for I_G. The impact of variation of g_s in the shade and in the sun on the CWSIs were the same, except for I_G where the sensitivity to the variation of g_s was higher in the sun than in the shade (Fig. 6c, 6d).

3.6. Effect of environmental parameters and stomatal conductance on T_{dry}, T_{wet}, T_L – Results of Morris method

Figure 7 summarizes the results of the sensitivity analysis based on the Morris method for T_{dry}, T_{wet} and T_L in sunny and shaded conditions. Unsurprisingly, T_{dry}, T_{wet} and T_L were principally driven by T_{air} (highest μ^*) in the sun ($\mu^* > 17$; Fig. 7a, 7c, 7e) and shade ($\mu^* > 21$; Fig. 7b, 7d, 7f). The influence of T_{air} on these three variables was approximately linear because the magnitude of σ was at least an order of magnitude less than μ^* (Menberg *et al*., 2016). In the sun σ/μ^* for T_{air} was 0.05, 0.11 and 0.11, and in the shade σ/μ^* was 0.03, 0.07 and 0.04 for T_{dry}, T_{wet} and T_L respectively. This result was in agreement with the curves obtained from the OAT method shown in Fig. 2a, 2b, which suggested an approximately linear relationship between surface temperatures and T_{air}. In the shade, the parameters RH, g_s, PAR and u had a lower effect ($\mu^* < 7$) than T_{air} ($\mu^* > 15$). In the sun, T_{dry} and T_L were significantly influenced by PAR ($\mu^* \approx 18$ for T_{dry} and $\mu^* \approx 11$ for T_L) and more weakly influenced by the other parameters (RH, g_s, u). Additionally, T_{wet} was weakly influenced by parameters other than T_{air} in the sun ($\mu^* < 7$; Fig. 7c). Except for T_{air}, the effects of the parameters on the models' outputs in the sun and shade were monotonic or almost monotonic ($0.1 < \sigma/\mu^* < 0.7$; Fig. 7a-f), which was in agreement with the curves obtained from the OAT method shown in Fig. 3-6 (a, b). u showed the highest value of σ (Fig. 7), which corresponds to the highly nonlinear curves from the OAT method shown in Fig. 5.

1.1. Effect of environmental parameters and stomatal conductance on CWSIs – Results of Morris method

Figure 8 summarizes the results of the sensitivity analysis based on the Morris method for $CWSI_1$, $CWSI_2$, $CWSI_3$ and I_G in sunny and shaded conditions. Although T_{air} was the most important parameter for T_{dry}, T_{wet}, and T_L, this was not the case for the CWSIs. In the sun, $CWSI_1$ was primarily influenced by u and g_s ($\mu^* = 0.114$ and

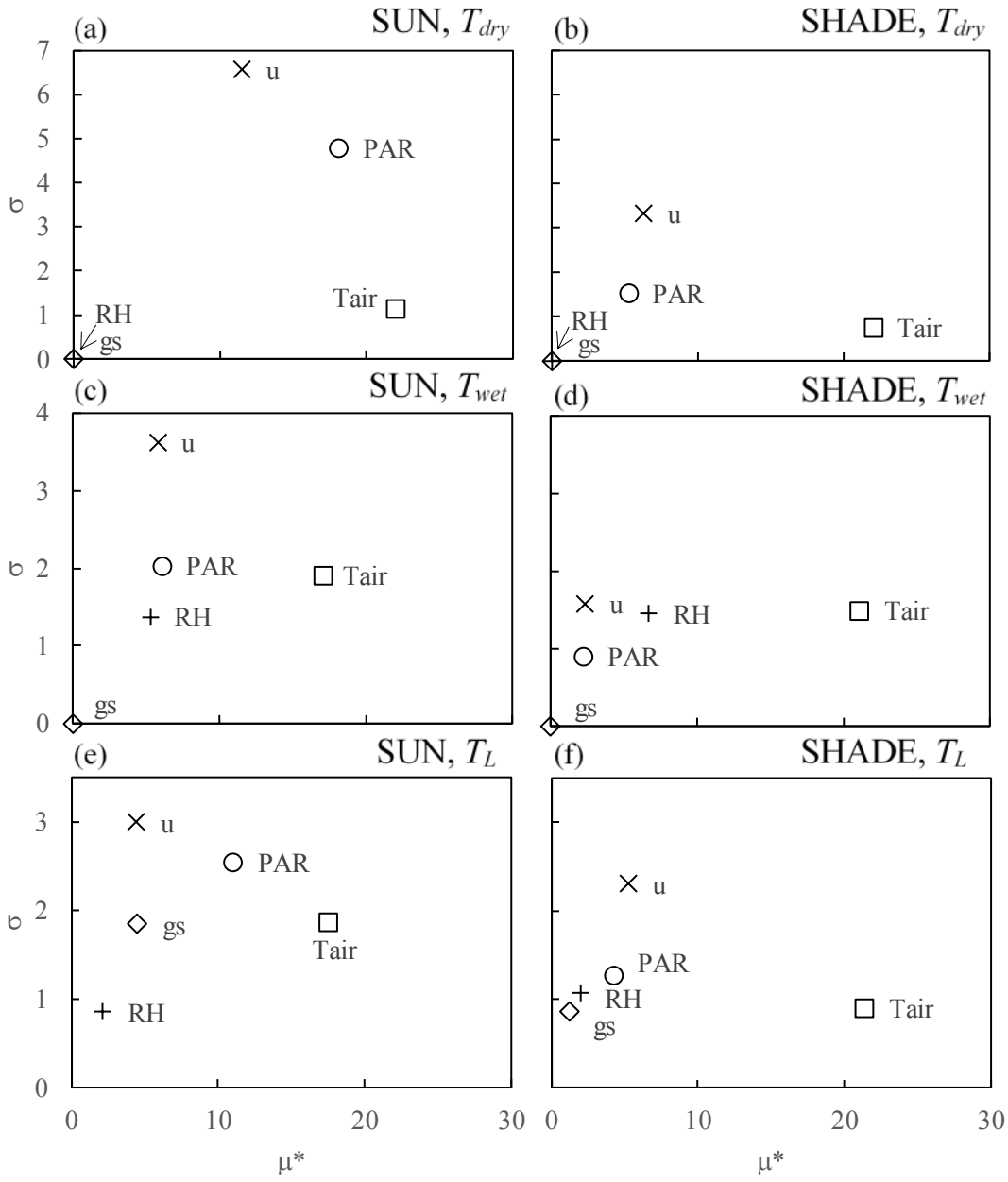

Fig.7: *Global sensitivity analysis of temperature using the Morris method. Mean (μ*) and standard deviation (σ) of the elementary effects of T_{air}, RH, PAR, u, and g_s on T_{dry} (a, b), T_{wet} (c, d) and T_L (e, f) in the sun (a, c, e) and shade (b, d, f).*

0.113, respectively) and secondarily by *PAR* (μ* = 0.09) (Fig. 8a). Their effects on $CWSI_1$ were monotonic (0.1 < σ/μ* < 0.5). Shady conditions decreased the impact of *u*, g_s, *PAR* and T_{air} but increased the effect of *RH* (Fig. 8e). Their effects remained approximately linear and monotonic, except for *u* in which σ/μ* > 1 which suggests that this parameter exhibit either non-linear behavior, interaction effects with other parameters, or both. $CWSI_2$ was driven mainly by g_s and secondarily by *u* in the sun (highest μ* of 0.312 and 0.268, respectively; Fig. 8b) and by *u* in the shade (μ* = 36.1; Fig. 8f). In the sun, the effect of all parameters was monotonic or almost monotonic (0.1 < σ/μ* < 0.6; Fig. 8b). In the shade, all parameters showed a ratio σ/μ* > 1 which suggested that the parameters exhibited either non-linear behavior, interaction effects with other parameters, or both. In the sun, all parameters had a similar influence on $CWSI_3$, and their effects were monotonic or almost monotonic (0.1 < σ/μ* < 0.7; Fig. 8c). In the shade, $CWSI_3$ was driven mainly by *RH* and secondarily by T_{air}. The other parameters had a small effect on $CWSI_3$. *RH* and T_{air} had monotonic or almost monotonic effects (0.1 < σ/μ* < 0.7; Fig. 8g).

Finally, I_G was driven primarily by g_s in the sun and secondarily by *u*. The other parameters had a minimal influence on the value of I_G (μ* < 1). In the shade, I_G was driven primarily by *u* (μ* = 25.1). The other parameters had a relatively small impact (μ* < 8). In the shade, the effects of all parameters were monotonic or almost monotonic (0.1 < σ/μ* < 1). In the sun, they had a ratio σ/μ* >> 1 which suggested that the parameters exhibited either non-linear behavior, interaction effects with other parameters, or both.

2. DISCUSSION

The use of leaf temperature and crop water stress indices to evaluate the water status of plants and manage irrigation requires consideration of ambient environmental factors, and interpretation requires a linkage to the stomatal conductance. Accordingly, we will first discuss the results of the two sensitivity analyses conducted in this study based the effects of environmental conditions and the stomatal conductance on T_{dry}, T_{wet}, T_L and four CWSIs. The sensitivity analysis results were used to compare the different CWSIs and ultimately assess the theoretical performance of the CWSIs.

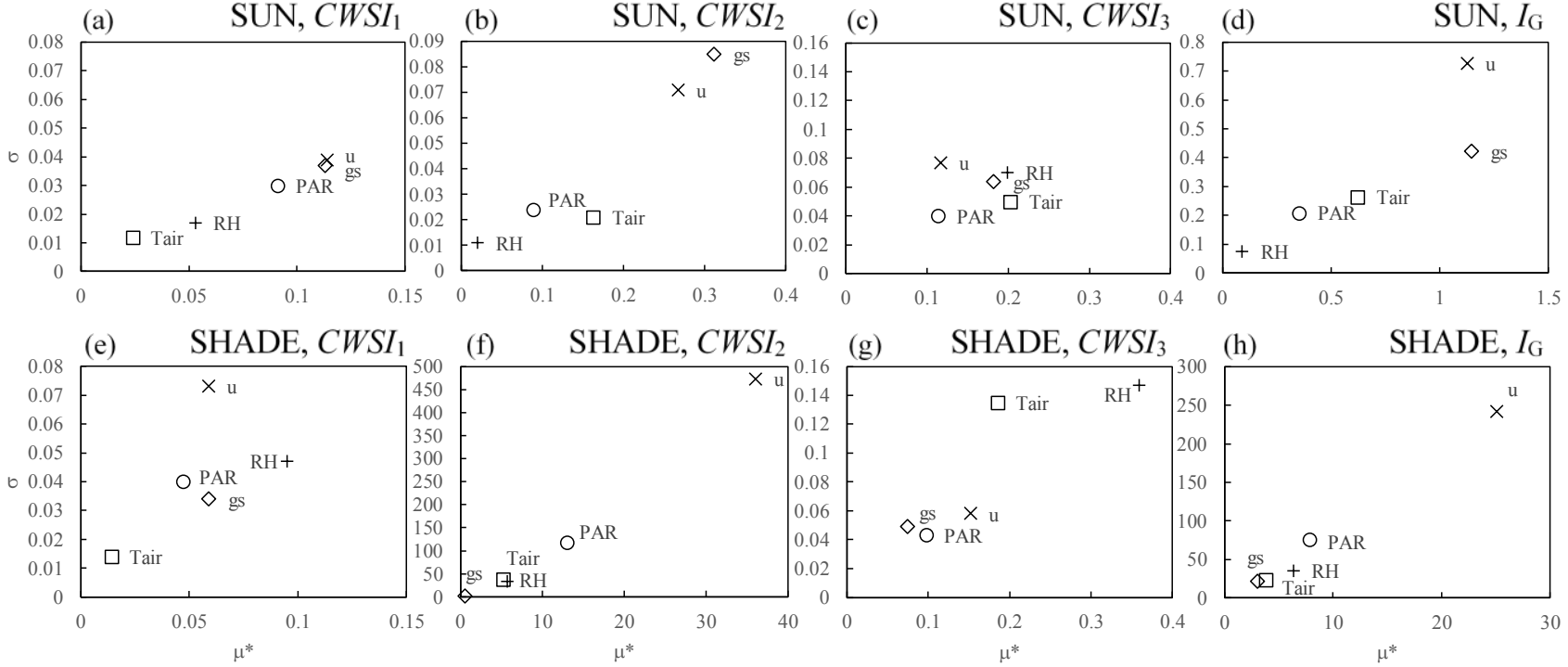

Fig.8: *Global sensitivity analysis of CWSIs using the Morris method. Mean (μ*) and standard deviation (σ) of the elementary effects of T_{air}, RH, PAR, u, and g_s on $CWSI_1$ (a, e), $CWSI_2$ (b, f), $CWSI_3$ (c, d) and I_G (d, h) in the sun (a, b, c, d) and shade (e, f, g, h).*

2.1. Local vs. global sensitivity analysis methods

The advantage of the analysis based on the Morris method is that it provides a global view by examining parameter interactions, which is not taken into account by the OAT method. In general, the OAT method provided insight into the magnitude of the effect of the input parameters (T_{air}, RH, PAR, u, and g_s) on the models' outputs (T_{dry}, T_{wet}, T_L, $CWSI_1$, $CWSI_2$, $CWSI_3$ and I_G), which Morris' method did not provide. Thus, the use of these two methods for sensitivity analysis provided complementary information.

2.2. Effect of environmental parameters and stomatal conductance on T_{dry}, T_{wet} and T_L

The sensitivity analysis showed that increasing PAR (*i.e.*, from shady to sunny conditions) increases the interactions between environmental parameters that influence T_{dry}, T_{wet} and T_L models because their σ increases relative to μ* (Fig. 7). T_{dry} was more sensitive than T_{wet} and T_L to PAR variation, although PAR still had a significant effect on T_{wet} and T_L (Fig. 4a, 4b, 7a, 7b). The sensitivity of leaf temperature to PAR was highlighted by Agam *et al.* (2013) and Jones *et al.* (2009). Agam *et al.* (2013) observed that variation in CWSI due to abrupt changes in radiation intensity was much larger in water-stressed trees compared to well-watered trees. In their experiments, when the radiation flux decreased from 700 to 200 W m^{-2}, temperatures of well-watered and stressed trees declined by 2 °C and 4.5 °C respectively, which is comparable to the reductions found by Jones *et al.* (2009).

Not surprisingly, the sensitivity analysis also showed that T_{air} has a strong effect on leaf temperatures (Woods *et al.*, 2018). However, unlike Woods *et al.* 2018, the analysis herein indicated that leaf temperature was most sensitive to air temperature rather than wind speed. It is possible that this is because they considered a range of wind speeds from 0 to 5 m s^{-1} along with a linear model for boundary-layer conductance that does not saturate at large wind speeds. In the shade, T_{dry}, T_{wet} and T_L were all dominated by the air temperature. This would indicate that sunny conditions are likely necessary to capture the effects of water status within temperature measurements because temperatures are not sensitive to g_s in the shade under typical conditions. Intuitively, this makes sense because increasing the radiative term in the energy balance amplifies the latent cooling term and thus the sensitivity of temperature to g_s. Previous work has used the level of variability in leaf temperature within a thermal image as a measure of water stress (Fuchs 1990; Jones *et al.* 2002;

González-Dugo *et al*. 2006), which is based on the principle that varying leaf angles creates variability in radiation, and that the sensitivity of leaf temperature to radiation increases with increasing water stress. The results of the present study would tend to support this idea, but also suggests that the discrepancy between the temperature of sunlit and shaded leaves within a thermal image increases with increasing water stress, and thus the level of temperature variability is also likely to capture this effect.

2.3. Effect of environmental parameters and stomatal conductance on the four CWSIs

The ultimate goal in formulating a CWSI is to derive an appropriate normalization of the measured leaf temperature that removes the impacts of ambient environmental conditions (namely *PAR*, *RH*, T_{air}, and *u*) and leaves only a dependence on g_s and thus water stress. While many CWSIs have been previously proposed, their effectiveness at performing this normalization has typically not been directly investigated theoretically. Jones (1999) examined the impact of *u* on several CWSIs including I_G and found that *u* had a significant influence on all CWSIs considered, which was also the case for all CWSIs investigated in this work (Fig. 8). Similarly, O'Toole and Hatfield (1983) found $CWSI_2$ to be very sensitive to *u*, which made estimating the CWSI from meteorological measurements problematic in some cases. For both $CWSI_2$ and I_G, the most important parameters (in the sun) were *u* and g_s with all other parameters playing a lesser role. Since the boundary-layer conductance g_H depends only on *u*, ang g_s and g_H together control the water flux, it makes sense that these CWSIs should be most sensitive to *u* and g_s. In contrast, under sunny conditions $CWSI_1$ was most sensitive to *u*, g_s, and *PAR*, and $CWSI_3$ was sensitive to all parameters. This result indicates that the normalizations used in $CWSI_1$ and $CWSI_3$, which use only one of either T_{wet} or T_{dry}, were ineffective at removing sensitivity of the CWSI to environmental conditions. Intuitively, one would expect that effective normalization would require both T_{wet} and T_{dry} in order to account for both the effects of radiation and convection (T_{dry}) as well as evaporation (T_{wet}) on the leaf temperature T_L. However, recent work by (Poirier-Pocovi *et al., submitted*) found that both T_{wet} and T_{dry} could be easily and accurately estimated from the temperature of a dry piece of green paper under a wide range of environmental conditions, which suggests that a proper normalization may not necessarily require an evaporating reference surface. The Morris sensitivity analysis (Fig. 7) may support this idea, as it indicated that T_{wet} was determined mainly by T_{air}, and only to a lesser extent by *RH*. If this is indeed the

case that T_L is not particularly sensitive to *RH*, one could reasonably expect that $CWSI_1$, which normalizes using only T_{dry}, would perform well. While $CWSI_1$ does a fairly good job at removing the effect of *RH*, it increased sensitivity to *PAR* in comparison with $CWSI_3$ and I_G. This could be because T_{dry} is also very sensitive to *PAR* (Fig. 7), and thus basing the CWSI normalization (particularly the denominator) on only T_{dry} appears to increase its sensitivity to *PAR*.

In shady conditions, all CWSIs performed poorly, with relatively low sensitivity to g_s and high sensitivity to all environmental parameters. Agam *et al.* (2013) also observed that $CWSI_2$ had a much weaker correlation with g_s under shady versus sunny conditions. In the absence of strong radiation forcing, the leaf temperature is primarily determined by the air temperature (Fig. 7) and thus evaporative cooling plays a lesser role. As such, leaf temperature is generally not likely to be a good indicator of plant water status as inferred through g_s.

Interestingly, in shady conditions I_G was highly sensitive to *u*, with all other parameters playing a lesser role. Because of this, it is possible that some variation of I_G in the shade could be used to develop a normalization that removes the strong and undesirable effect of *u* in $CWSI_2$ and I_G. However, this requires experimental testing since, although I_G is deemed "sensitive" to *u* in the shade in a relative sense based on the Morris sensitivity parameters, all energy fluxes are relatively small in the shade and thus it is unclear whether the signal from *u* would be robust. However, the results of the OAT analysis suggest that T_L has high absolute sensitivity to *u* in the shade, in fact more so than in the sun (Fig. 5).

3. CONCLUSION AND RECOMMENDATION

Our results suggest several recommendations for infrared measurement of leaf temperature and the use of CWSIs to estimate plant water status. We considered the best CWSI to be one that has maximal sensitivity to g_s and minimal sensitivity to environmental conditions, which in terms of the Morris sensitivity analysis, would be the CWSI in which the μ* value of g_s was largest relative to the μ* of environmental variables. Additionally, if a variable's σ value is comparable in magnitude to its μ* value, caution is required in interpreting its sensitivity as it could indicate the presence of non-linearities or interactions that could make results dependent on the choice of parameter ranges.

$CWSI_2$ and I_G showed similar performance in terms of the sensitivity analysis. Both were most sensitive to g_s and u, with other environmental variables playing a lesser role. One could argue that I_G is preferable based on the desirable trait that it is proportional to g_s and thus making interpretation with respect to plant water status more straight-forward. However, $CWSI_2$ was slightly more sensitive to g_s in comparison with other variables than I_G including u. Additionally, the ratio of σ/μ^* for u in I_G is relatively large indicating the possibility of a non-linear impact, whereas $CWSI_2$ has the desirable trait that all environmental variables appear to have a linear impact. Future work could further improve calculation of CWSIs by focusing on developing a normalization that can remove the impact of u.

According to the results of the sensitivity analysis, it is not recommended measure CWSIs in shaded conditions, but rather to perform measurements in full sun (*i.e.*, PAR>700 μmol m^{-2} s^{-1}). The lack of strong radiative forcing increases the impact of other environmental variables such as T_{air} and decreases the impact of g_s.

ACKNOWLEDGEMENT

This work was supported by the Almond Board of California, and by USDA National Institute of Agriculture Hatch project 1013396 (BNB). We acknowledge Dr. A. Volder for providing the experimental plant material.

REFERENCES

Agam, N., Cohen, Y., Alchanatis, V., Ben-Gal, A. 2013. How sensitive is the CWSI to changes in solar radiation? *Int. J. Remote Sens.* 34(17), 6109-6120. https://doi.org/10.1080/01431161.2013.793873

Campbell, G.S., Norman, J.M. 1998. An introduction to environmental biophysics. 2nd edition. New York: Springer. pp 286

Daudet, F.A., Le Roux, X., Sinoquet, H., Adam, B. 1999. Wind speed and leaf boundary layer conductance variation within tree crown: Consequences on leaf-to-atmosphere coupling and tree functions. *Agric. For. Meteorol.* 97, 171-185. https://doi.org/10.1016/S0168-1923(99)00079-9

Eaton, J.W., Bateman, D., Hauberg, S., Wehbring, R. 2018. GNU Octave version 4.4.1 manual: a high-level interactive language for numerical computations. URL: https://www.gnu.org/software/octave/doc/v4.4.1/

Egea, G., González-Real, M.M., Baille, Nortes, P.A., Sánchez-Bel, P., Domingo, R. 2009. The effects of contrasted deficit irrigation strategies on the fruit growth and kernel quality of mature almond trees. *Agr. Water Manage*. 96(11), 1605-1614. https://doi.org/10.1016/j.agwat.2009.06.017

Fuchs, M. 1990. Infrared measurement of canopy temperature and detection of plant water stress. *Theor. Appl. Climatol.* 42, 253-261. https://doi.org/10.1007/BF00865986

García-Tejero, I.F., Rubio, A.E., Viñuela, I., Hernández, A., Gutiérrez-Gordillo S., Rodríguez-Pleguezuelo, C.R., Durán-Zuazo, V.H. 2018. Thermal imaging at plant level to assess the crop-water status in almond trees (cv. Guara) under deficit irrigation strategies. *Agr. Water Manage.* 208, 176-186. https://doi.org/10.1016/j.agwat.2018.06.002

García-Tejero, I.F., Romero-Vicente, R., Jiménez-Bocanegra, J.A., Martínez-García, G., Durán-Zuazo, V.H., J.L. Muriel-Fernández. 2010. Response of citrus trees to deficit irrigation during different phenological periods in relation to yield, fruit quality, and water productivity. *Agr. Water Manage*. 97, 689-699. https://doi.org/10.1016/j.agwat.2009.12.012

Goldhamer, D., Beede, R. 2004. Regulated deficit irrigation effects on yield, nut quality and water-use efficiency of mature pistachio trees. *J. Hortic. Sci. Biotech.* 79(4), 538-545. https://doi.org/10.1080/14620316.2004.11511802

González-Dugo, M.P., Moran, M.S., Mateos, L., Bryant, R. 2006. Canopy temperature variability as an indicator of crop water stress severity. *Irrigation Sci.* 24(4), 233-240. https://doi.org/10.1007/s00271-005-0022-8

Grant, O.M., Tronina, Ł., Jones, H.G., Chaves, M.M. 2007. Exploring thermal imaging variables for the detection of stress responses in grapevine under different irrigation regimes. *J. Exp. Bot.* 58(4), 815-825. https://doi.org/10.1093/jxb/erl153

IPCC. 2014. Climate Change 2014: Synthesis Report. Contribution of Working Groups I, II and III to the Fifth Assessment Report of the Intergovernmental Panel on Climate Change [Core Writing Team, R.K. Pachauri and L.A. Meyer (eds.)]. IPCC, Geneva, Switzerland, pp. 151.

Idso, S.B. 1982. Non-water stressed baselines: a key to measuring and interpreting plant water stress. *Agr. Meteorol*. 27, 59-70. https://doi.org/10.1016/0002-1571(82)90020-6

Jacksons, R.D., Idso, B., Reginato, R.J., Pinter, P.J., JR., 1981. Canopy temperature as a crop water stress indicator. *Water Resour. Res*. 17(4), 1133-1138. https://doi.org/10.1029/WR017i004p01133

Jones, H.G., Stoll, M., Santos, T., De Sousa, C., Chaves, M.M., Grant, O.M., 2002. Use of infrared thermography for monitoring stomatal closure in the field: application to grapevine. *J.Exp. Bot.* 53(378), 2249-2260. https://doi.org/10.1093/jxb/erf083

Jones, H.G., Serraj, R., Loveys, B.R., Xiong, L.Z., Wheaton, A., Price, A.H. 2009. Thermal infrared imaging of crop canopies for the remote diagnosis and quantification of plant responses to water stress in the field. *Funct. Plant Biol*. 36, 978-989. https://doi.org/10.1071/FP09123

Jones, H.G., Aikman, D., McBurney, T.A., 1997. Improvements to infrared thermometry for irrigation scheduling in humid climates. *Acta Hortic.* 449, 259-266. https://doi.org/10.17660/ActaHortic.1997.449.37

Jones, H.G., 1999. Use of infrared thermometry for estimation of stomatal conductance in irrigation scheduling. *Agr. Forest Meteorol*. 95, 135-149. https://doi.org/10.1016/S0168-1923(99)00030-1

Menberg, K., Heo, Y., Choudhary, R. 2016. Sensitivity analysis methods for building energy models: Comparing computational costs and extractable information. *Energ. Buildings*. 133, 433-445. http://dx.doi.org/10.1016/j.enbuild.2016.10.005

Morris, M.D. 1991. Factorial sampling plans for preliminary computational experiments. *Technometrics*, 33, 161-174. https://doi.org/10.1080/00401706.1991.10484804

Nanda, M.K., Giri, U., Bera, N. 2018. Canopy Temperature-Based Water Stress Indices: Potential and Limitations. *In*: Bal S., Mukherjee J., Choudhury B., Dhawan A. (eds) Advances in Crop Environment Interaction. Springer, Singapore. https://doi.org/10.1007/978-981-13-1861-0_14

O'Toole, J.C., Hatfield, J.L. 1983. Effect of wind on the crop water stress index derived by infrared thermometry. *Agron. J.* 75, 811-817. https://doi.org/10.2134/agronj1983.00021962007500050019x

Patumi, M., D'Andria, R., Fontanazza, G., Morelli, G., Giorio, P., Sorrentino, G. 1999. Yield and oil quality of intensively trained trees of three cultivars of olive (*Olea europaea* L.) under different irrigation regimes. *J. Hortic. Sci. Biotech*. 74(6), 729-737. https://doi.org/10.1080/14620316.1999.11511180

Poirier-Pocovi, M., Volder, A., Bailey, B.N. (submitted). Modeling of wet and dry reference temperatures for calculating crop water stress indices from infrared thermography. *Agr. Water Manage*.

Pianosi, F., Sarrazin, F., Wagener, T. 2015. A Matlab toolbox for Global Sensitivity Analysis. *Environ. Model. Softw*. 70, 80-85. https://doi.org/10.1016/j.envsoft.2015.04.009

Piedallu, C., Gégou, J.C. 2007. Multiscale computation of solar radiation for predictive vegetation modelling. *Ann. For. Sci*. 64, 899-909. https://doi.org/10.1051/forest:2007072

Qiu, G.Y., Momii, K., Yano, T., 1996. Estimation of plant transpiration by imitation leaf temperature - Theoretical consideration and verification (I). *Transactions of JSIDRE*. 183, 47-56. https://doi.org/10.11408/jsidre1965.1996.401

Sager, J.C., Mc Farlane, J.C. 1997. Chapter 1: Radiation. *In*: Langhans, R.W., Tibbitts, T.W. (eds) Plant growth chamber handbook. North Central Regional Research Publication No. 340, Iowa Agriculture and Home Economics Experiment Station Special Report No. 99. IOWA State University of Science and technology. pp. 240.

Sicart, J. E., Pomeroy, J.W., Essery,R., Hardy, J. 2003. Snowmelt in a Canadian spruce forest: A sensitivity study to the canopy cover. Proceeding of the 60th Eastern Snow Conference, Sherbrooke, QC, Canada, Eastern Snow Conference, 99–110.

Susorova, I., Angulo, M., Bahrami, P., Stephens, B. 2013. A model of vegetated exterior facades for evaluation of wall thermal performance. *Building and Environment*. 67, 1-13. http://dx.doi.org/10.1016/j.buildenv.2013.04.027

Woods, H.A., Saudreau, M., Pincebourde, S. 2018. Structure is more important than physiology for estimating intra-canopy distributions of leaf temperatures. *Ecol. Evol.* 8, 5206-5218. https://doi.org/10.1002/ece3.4046

Publication 2

ORIGINAL PAPER – SUBMISSION PROCESS *IN PROGRESS*.
Result of the first submission: moderate modifications

Modeling of reference temperatures for calculating crop water stress indices from infrared thermography

Magalie Poirier-Pocovi[a], Astrid Volder[a], Brian N. Bailey[a]*

*For correspondence, E-mail: mdpoirier@ucdavis.edu
[a] University of California, Davis, Department of Plant Sciences, One Shields Avenue, Davis, California 95616-8571, U.S.A.

Highlights:

- Wet reference temperature was well-predicted based on temperature of a dry surface.
- Wet and dry leaf temperatures were linearly related to the temperature of green paper.
- CWSI could be calculated by modeling the wet and dry leaf temperature.
- The same reference can be used in both the sun and shade and for different species.

Agricultural Water Management (2020) xxx, xxx-xxx
https://doi.org/

ABSTRACT

Leaf temperature (T_L) is tightly coupled with the rate of transpirational water loss from the leaf. The temperatures of wet and dry reference leaf surfaces (T_{wet} and T_{dry}, respectively) are commonly used to normalize temperature measurements for current environmental conditions and then calculate a crop water stress index (CWSI).

Since it is often impractical to directly measure T_{dry} and T_{wet}, the goals of this work were to: i) determine a suitable artificial reference surface that makes application of the CWSI faster and easier in the field, ii) develop a model for T_{dry} and T_{wet} based on the reference surface temperature that allows for calculation of standard CWSIs, iii) test the technique for a range of weather conditions and tree species, and iv) analyze the sensitivity of these two models to T_{dry} and $T_{wet,}$ and their impact on the estimation of four different CWSIs.

Our results showed that both T_{dry} and T_{wet} are linearly related to the thermal temperature of green paper across a wide range of environmental conditions. Although there was a significant effect of the light conditions on T_{dry} and T_{wet}, the same models could be used in both the sun and shade to relate T_{dry} and T_{wet} to T_{ref}. Moreover, results indicated that a new CWSI dependent only on T_L and T_{wet} was least sensitive to errors in T_{wet}, but most sensitive to T_L.

Keywords: Irrigation scheduling, crop-water status, thermal imaging, *Prunus dulcis*

1. INTRODUCTION

Thermal imaging can be used to measure leaf or canopy temperatures, which can then be used to estimate plant water status and therefore aid in irrigation scheduling of various crops (Jones *et al.*, 2002; Ballester *et al.*, 2013; Struthers *et al.*, 2015; Gerhards *et al.*, 2016; Craparo *et al.*, 2017; García-Tejero *et al.*, 2017; Gutiérrez *et al.*, 2018). Plants lose large amounts of water through their stomatal pores while taking up CO_2 for photosynthesis. When plant water availability declines, stomata close to conserve water (Hopkins, 2003), reducing evaporative cooling and increasing leaf temperature. Thermal imaging can then be employed to measure leaf temperature responses to water stress conditions, and thereby infer impacts on transpiration and stomatal behavior. In addition, thermal imaging provides measurements of the temperature of whole canopy, and thus has the potential for fast spatio-temporal measurements and water status assessment on a whole plant basis. However, the interpretation of thermal imagery is complicated by the fact that it aggregates many leaves with different environmental conditions and orientations, which may affect the measurement.

In addition to transpiration rate, canopy temperature is also strongly influenced by the local environmental conditions (e.g., air temperature, wind speed, radiation; Campbell and Norman, 1998). In order to remove the effects of environmental conditions from leaf temperature measurements and isolate water status effects, the temperature must be normalized, which is commonly performed using both well-watered and non-transpiring reference crop temperatures (Idso, 1982). The well-watered and non-transpiring crop temperatures, respectively, provide a theoretical lower and upper bound for possible actual leaf surface temperatures given identical environmental conditions. These reference temperatures allow for the formulation of a dimensionless temperature index, commonly called the "crop water stress index" or CWSI. Many CWSIs have been proposed that use some combination of wet and dry reference surface temperatures, each with the goal of increasing sensitivity of the index to water stress while decreasing sensitivity to environmental conditions (e.g., Jones, 1999; Grant *et al.*, 2007; Costa *et al.*, 2013; García-Tejero *et al.*, 2016; Cohen *et al.*, 2017; Poirier-Pocovi and Bailey, 2020).

While theoretically convenient, it is rarely possible in practice to have access to well-watered and non-transpiring crop temperatures for the same crop under identical

environmental conditions. Jones *et al*. (2002) thus compared various types of surfaces to replace the reference crop temperatures, and concluded that the temperatures of real leaves from the same plant sprayed with water (T_{wet}) or covered in petroleum jelly to stop transpiration (T_{dry}), provided effective reference temperatures because of the similar radiometric and aerodynamic properties to the actual leaves being studied. Since wet reference leaves dry out quickly, Maes *et al*. (2016) presented and evaluated a new artificial wet reference surface that could stay wet for several days. The reference leaf was fabricated by knitting a cotton cloth around a steel wire frame, where the bottom part of the cloth was put in a water bottle wrapped with aluminum foil to act as a wick.

To avoid having to perform reference temperature measurements altogether, previous workers have modeled the values of T_{wet} and T_{dry}, either arbitrarily by adding X °C (an empirical estimate dependent on vapor pressure deficit or a constant offset) to the air temperature (Cohen *et al*., 2005, 2017; Bellvert *et al*., 2015), or theoretically by using the energy balance equation (Alchanatis *et al*., 2010; Möller *et al*., 2007). The theoretical energy balance approach requires knowledge of complex parameters (e.g., net radiation of the leaf, the resistance to convective heat transfer, the slope of the saturation vapor-pressure curve). In practical application of this approach, the experimenters or producers are often unable to provide input variables in the model without expensive equipment that requires technical expertise.

The primary objective of this work was to determine a surrogate reference surface temperature that could be used along with a model to more easily estimate T_{dry} and T_{wet} values without any additional measurements. Any error in the estimation of T_{dry} and T_{wet} will propagate to the calculation of the CWSI. Thus, we studied four different CWSI formulations, including two new CWSIs, to determine whether certain CWSI formulations were able to minimize sensitivity to errors in the estimation of T_{dry} and T_{wet} while maximizing sensitivity to water status. The specific novel aims of this study were (i) to develop a model that relates the temperature of a suitable artificial reference surface (T_{ref}) to T_{dry} and T_{wet}, thus making the application of a CWSI faster and easier in the field, (ii) to test the model for a wide range of weather conditions and tree species, and (iii) to analyze the sensitivity of these models for T_{dry} and T_{wet} and their impact on the estimation of four different CWSIs.

2. MATERIALS AND METHODS

2.1 Plant material

This study was performed in 2018 on twelve almond trees (*Prunus dulcis* Mill. cv. 'Non Pareil', grafted onto Krymsk 86 rootstock, n = 12) that were four-years-old in an experimental orchard at the University of California, Davis, located in Northern California (average altitude: 23 m; 38°32'16" N, 121°47'42" W). At the experimental site, full bloom occurred during week 7 of the calendar year (16 Feb. 2018). The almond trees were watered once per week (between Saturday and Sunday) with a micro sprinkler system.

To verify the general applicability of the model, several additional woody species with hypostomatous leaves were selected: *Prunus persica*, *Nerium oleander*, *Quercus sp.*, *Olea europaea* L. and *Ulmus* hybrid 'Frontier'. These species were all located on the campus of the University of California, Davis within a 3.7 km radius of the above-mentioned almond orchard.

2.2 Sampling strategy

A number of thermal measurements were performed on six fully developed leaves with approximately the same orientation and size for each of the tree species: three in the shaded zone inside the canopy ($10 < PAR < 300$ µmol photons m^{-2} s^{-1}), and three in the sunny zone outside the canopy ($700 < PAR < 1750$ µmol photons m^{-2} s^{-1}). On each day of measurements, six new leaves were selected. Measurements were performed during four periods: 15 June 2018 (Julian Day Number (JDN) 166, on *U.* hybrid 'Frontier' only), from 18 June 2018 to 22 June 2018 (JDN 169-173, on *P. persica*, *N. oleander*, *Q. sp.*, and *O. europa* L., *U.* hybrid 'Frontier'), from 30 July 2018 to 3 August 2018 (JDN 211-215, all species) and from 27 August 2018 to 31 August 2018 (JDN 239-243, *P. dulcis* only). All measurements were collected uniformly in the morning between 9:00 am and 12:00 pm. We chose this time period because the environmental conditions covered a wide range of values over a relatively short time period. This high variability was desirable because it increased the domain of model validity.

2.3 Thermal imaging

Leaf temperatures were measured using thermal images obtained using a FLIR camera (FLIROne® Pro for iOS, FLIR, Wilsonville, OR, USA) that was connected to an iPhone 6 (Apple, USA). The camera produces thermal images of 480 × 640 pixels

(*Horizontal* × *Vertical*), with an accuracy of ± 0.1 °C. Horizontal and vertical fields of view for the thermal images are 55° ± 1° and 43° ± 1°, respectively. For the same leaves, two thermal pictures were collected: one from the top surface and one from the bottom surface of the leaves. In order to maximize thermal contrast between the leaf and background while minimizing influence of the background on the temperature of the leaf, the background surfaces were chosen to be a sheet of black paper (Canford card 8.5"x11", Jet Black) for shady conditions, and "uncrumpled" aluminum foil for sunny conditions (Fig. 1).

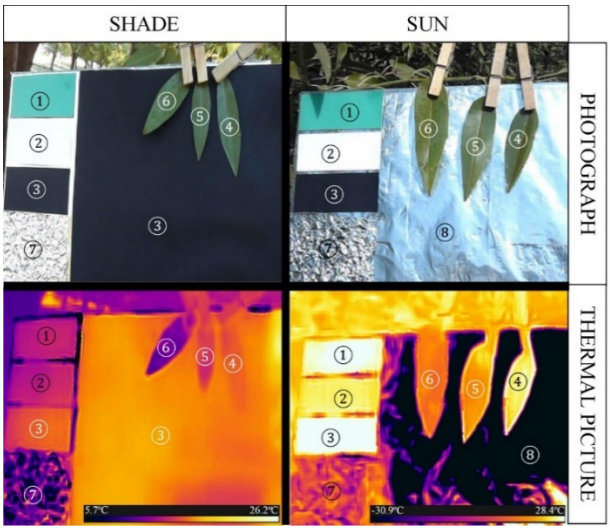

Fig. 1: *Illustration of the experimental apparatus for collecting thermal images in shady (a) and sunny (b) conditions, which consists of green (①), white (②) and black (③) reference surfaces, leaves to measure* T_{dry} *(④),* T_L *(⑤) and* T_{wet} *(⑥), crumpled (⑦) and uncrumpled (⑧) aluminum foil sheet. The real emissivity of the "uncrumpled" aluminum foil is very low (0.09 – 0.04; FLIR, 2017). Because we have taken emissivity values greater than 0.61 for all objects in the picture, the thermal temperature of the "uncrumpled" aluminum foil therefore appeared unrealistically low (-31 °C).*

The reflectance temperature required for calibration of the thermal image was estimated to be the radiative temperature of a "crumpled" aluminum foil sheet placed next to the object being viewed, with its emissivity set at 1.0. Thermal images were processed using FLIR Tools software (version 6.4.18039.1003, FLIR, Wilsonville, OR, USA). The effective leaf emissivity was measured using the method described in detail in the user's manual of FLIR ETS3xx series camera (FLIR®, 2017). The average emissivity from several replicate measurements yielded the following values: 0.87 for *P. persica* (n = 11), 0.61 for *P. dulcis* (n = 13), 0.81 for *U.* hybrid 'Frontier' (n = 6) and *Q. sp.* (n = 6), 0.94 for *N. oleander* (n = 6), and 0.98 for *O. europa* L (n =

6). The measured leaf emissivity value was also used for all objects in the picture to build the model. Although specifying the correct emissivity for each surface is important for accurate measurement of absolute temperature, the fact that the same emissivity was used for all surfaces in the image meant that the emissivity value cancels out when developing the model to relate the leaf temperature to reference temperatures in the image. It was verified that changing emissivity values had no effect on the final model results.

2.4 Wet and dry leaf reference surface temperature

The reference surfaces temperatures under wet and dry conditions were determined by measuring the temperature of an adjacent leaf that was sprayed with water on both sides approximately 1 min before the imaging. The dry leaf reference surface T_{dry} was prepared by covering an adjacent leaf in petroleum jelly (Vaseline, 100% pure petroleum jelly, Unilever, US) on both sides of the leaf (Jones *et al.*, 2002). For each picture, three adjacent leaves were chosen, two representing the reference surface temperature (T_{wet} and T_{dry}) and one representing the temperature of the leaf of interest (T_L).

Several types of surfaces were selected as candidates for the approximation of T_{wet} and T_{dry}. The temperatures of sheets of paper (T_{ref}) of color green ($T_{refgreen}$, Canford card 8.5"x11", Emerald Green), black (Canford card 8.5"x11", Jet Black) and white (Canford card 8.5"x11", Snow White) paper were measured to test their ability to represent the "true" wet and dry temperatures (Fig. 1).

2.5 Crop water stress indices

Several potential crop water stress indices (CWSIs) were considered in this study. The different formulations of the CWSI were based on different normalizations of T_L based on T_{wet} and T_{dry}. These different normalizations change the influence of the environmental conditions on the CWSI value (Poirier-Pocovi and Bailey, 2020), which could also change the impact of errors in estimation of T_{wet} and T_{dry} on the calculated CWSI.

A first CWSI based only on T_{dry} and T_L was calculated as follows (Poirier-Pocovi and Bailey, 2020)

$$CWSI_1 = \frac{T_{dry} - T_L}{T_{dry}}, \quad (1)$$

where T_{dry} is the temperature of a dry reference leaf surface (non-transpiring leaf, ºC) and T_L is the temperature of the leaf of interest (ºC). Since $T_{dry} \geq T_L$, $CWSI_1 \geq 0$, with

$CWSI_1$ = 0 for a non-transpiring leaf, and $CWSI_1$ increasing as the leaf becomes increasingly hydrated.

A second CWSI was calculated as follows (also called $CWSI_{NI/FI}$ by Grant *et al.*, 2007)

$$CWSI_2 = \frac{T_{dry} - T_L}{T_{dry} - T_{wet}}, \quad (2)$$

where T_{wet} is the temperature of a wet reference leaf surface (°C). Since $T_L \geq T_{wet}$ and $T_{dry} \geq T_L$, $0 \leq CWSI_2 \leq 1$ in theory. However, unless liquid water is present on the exterior of the leaf under investigation (e.g., rain, dew) or the vapor pressure deficit is zero, T_L will usually be significantly greater than T_{wet}, and thus $CWSI_2$ is unlikely to reach a value of 1 in a fully-irrigated crop.

A third CWSI based only on T_{wet} and T_L was calculated as follows (Poirier-Pocovi and Bailey, 2020)

$$CWSI_3 = \frac{T_L - T_{wet}}{T_{wet}}. \quad (3)$$

Using this approach, $CWSI_3 \geq 0$ in theory, with $CWSI_3$ increasing as the crop dries out.

Finally, a fourth CWSI derived by Jones *et al.*, 2002 is defined as follows

$$I_G = \frac{(T_{dry} - T_L)}{(T_L - T_{wet})}. \quad (4)$$

A strength of this formulation is that it is theoretically proportional to stomatal conductance (Jones *et al.*, 2002), thus making its interpretation in a relative sense straightforward. It also has the same lower theoretical bounds as $CWSI_2$, but has upper bounds of infinity (i.e., $0 \leq I_G \leq \infty$).

Between 9:00 am and 12:00 pm, the environmental conditions varied strongly and have a high influence on the real value of the CWSI. For this reason, the percentage of the variation of the CWSI is considered rather than the absolute value.

2.6 Meteorological data

Although not directly used in the calculation of CWSIs, local meteorological data were collected and reported to characterize the climate at the experimental site and ambient environmental conditions during the thermal measurements. Daily average relative humidity (RH, %), daily minimum and maximum air temperatures (min T_{air} and max T_{air}, °C) were obtained from weather station n°6 of the California Irrigation

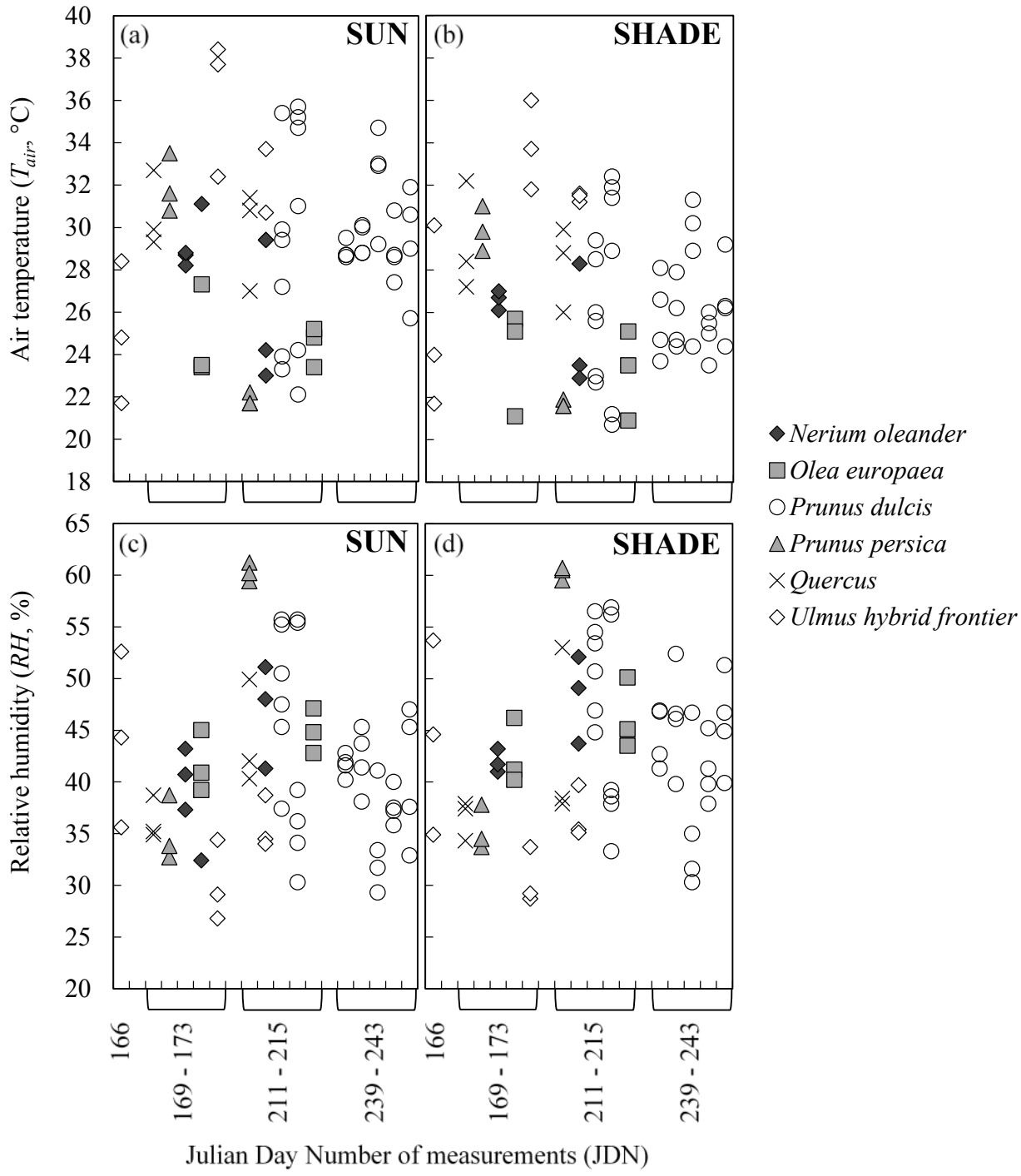

Fig. 2: *Air temperature (T_{air}; a) and relative humidity (RH; b) recorded adjacent to each individual leaf (data from the thermo-hygrometer probe) during each measurement period (JDN: Julian Day Number). Data are separated by species and light conditions (sunlit or shaded), but not by site. All data were recorded in the morning between 9 am and 12 pm.*

Management Information System (CIMIS) network (cimis.water.ca.gov), which was located about 1.6 km from the experimental site for *P. dulcis* and about 2.1 km from the other species. In order to characterize the range of environmental conditions under which the models for T_{wet} and T_{dry} were developed and tested, data were collected adjacent to the leaf. The air temperature (T_{air}, °C) and the relative humidity of the air adjacent to the leaf were measured a few seconds after the thermal imaging with a thermo-hygrometer probe for smartphones (model 800014, TFA® Dostmann GmbH & Co.KG, Wertheim, Germany) in order to characterize the environment in the vicinity of the leaf (Fig. 2, 5g, 5h), and to correct the thermal images for absorption of longwave radiation due to the atmosphere.

2.7 Statistical analysis

Linear and nonlinear regressions between T_{dry}, T_{wet} and the reference paper surface temperature (black, green or white), or T_{air} were fitted to the data using SIGMAPLOT version 13.0 for Windows (SPSS Inc., San José, CA, USA). The goodness-of-fit of the resulting regressions (models) were evaluated using the following three statistics:

(1) The coefficient of determination, adjusted for estimated parameters (Hill and Lewicki, 2007; Dincer and Topuz, 2015) to yield an unbiased value, R^2_{adj} and is defined as

$$R^2_{adj} = 1 - \frac{n-1}{n-(k+1)} \times (1 - R^2), \quad (5)$$

n is the sample size, k is the number of independent variables in the regression equation and R^2 is the coefficient of the determination defined as

$$R^2 = 1 - \frac{\sum_{i=1}^{n}(O_i - P_i)^2}{\sum_{i=1}^{n}(O_i - \grave{O})^2}, \quad (6)$$

n is the sample size, $\grave{O}$ is the mean of observed values, O_i and P_i are the i^{th} observed and i^{th} corresponding model-predicted variables, respectively.

(2) The index of agreement d is a standardized measure of the degree of model prediction error and is defined by Willmott (1982) as

$$d = 1 - \left[\frac{\sum_{i=1}^{n}(P_i - O_i)^2}{\sum_{i=1}^{n}(|P_i'| + |O_i'|)^2}\right], \quad (7)$$

$P_i' = P_i - \grave{O}$, $O_i' = O_i - \grave{O}$, and $0 \le d \le 1$. A value of 1 indicates perfect agreement, while 0 indicates a random relationship.

(3) The quadratic mean deviation estimated from measured values, or root mean squared error, RMSE (Janssen and Heuberger, 1995) and is defined as

$$RMSE = \sqrt{\frac{\sum_{i=1}^{n}(P_i - O_i)^2}{n}}. \quad (8)$$

JAMOVI (Version 0.9, free computer software, retrieved from https://www.jamovi.org) was used to compare the slopes and *y*-intercepts of the linear regressions with analysis of covariance (ANCOVA) (Engqvist, 2005). SIGMAPLOT version 13.0 for Windows (SPSS Inc., San José, CA, USA) was used to perform the normality test and to compare the means with adapted analysis of variance (ANOVA, Tukey test).

For model parameterization, we used three-quarters of the presented data for *P. dulcis* (three trees of *P. dulcis* were chosen at random (n = 96)). The rest of the data (the remaining tree of *P. dulcis* (n = 32)) and measurements from other species (*P. persica*, *N. oleander*, *Q. sp.*, *O. europaea*, *U. hybrid 'frontier'* (n = 102)) were used for a model validation. The models' predictive capacity was evaluated by performing validation based on data sets that were not used to parameterize the model (see above), and quantifying errors using the same three indices: R^2_{adj}, *d* and RMSE, hereafter referred to as the RMSE of prediction ($RMSE_P$) and *d* of the prediction (d_P), respectively.

2.8 Sensitivity analysis

Microsoft Excel was used to study the sensitivity of the CWSIs by changing one-factor-at-a-time (OFAT or OAT method), to see what effect this produces on the output (Pianosi *et al.*, 2016). This method involves changing one input variable, keeping others at their baseline (nominal) values, then, returning the variable to its nominal value, and repeating for each of the other inputs in the same way. For our models, we changed only the thermal temperature of the reference surface measured by thermal imaging to see its effect on the outputs (T_{dry}, T_{wet} and CWSI). T_L remained fixed in the OAT method and its value is the measured data.

RStudio version 1.1.463 was used to calculate the sensitivity indices: the main (first-order) and the total effects of Sobol sensitivity analysis (Monte Carlo Estimation of Sobol' Indices (formulas of Martinez (2011) (Martinez, 2011; Baudin *et al.*, 2016)). For the parameters in the Sobol sensitivity analysis, we took the ranges of temperature values ([20 - 45] °C) that are typical for California, USA region where almond trees are cultivated. We assumed that the parameters used to calculate the CWSIs are independent. The number of model evaluations was equal to 10^6.

3. RESULTS

3.1 Air temperature and relative humidity during the experimental period

Variations of daily average relative humidity, daily minimum and maximum air temperatures (average *RH*, min T_{air} and max T_{air}) between 1 February 2018 (Julian Day Number, JDN 32) and 31 August 2018 (JDN 243) are shown in Fig. 3.

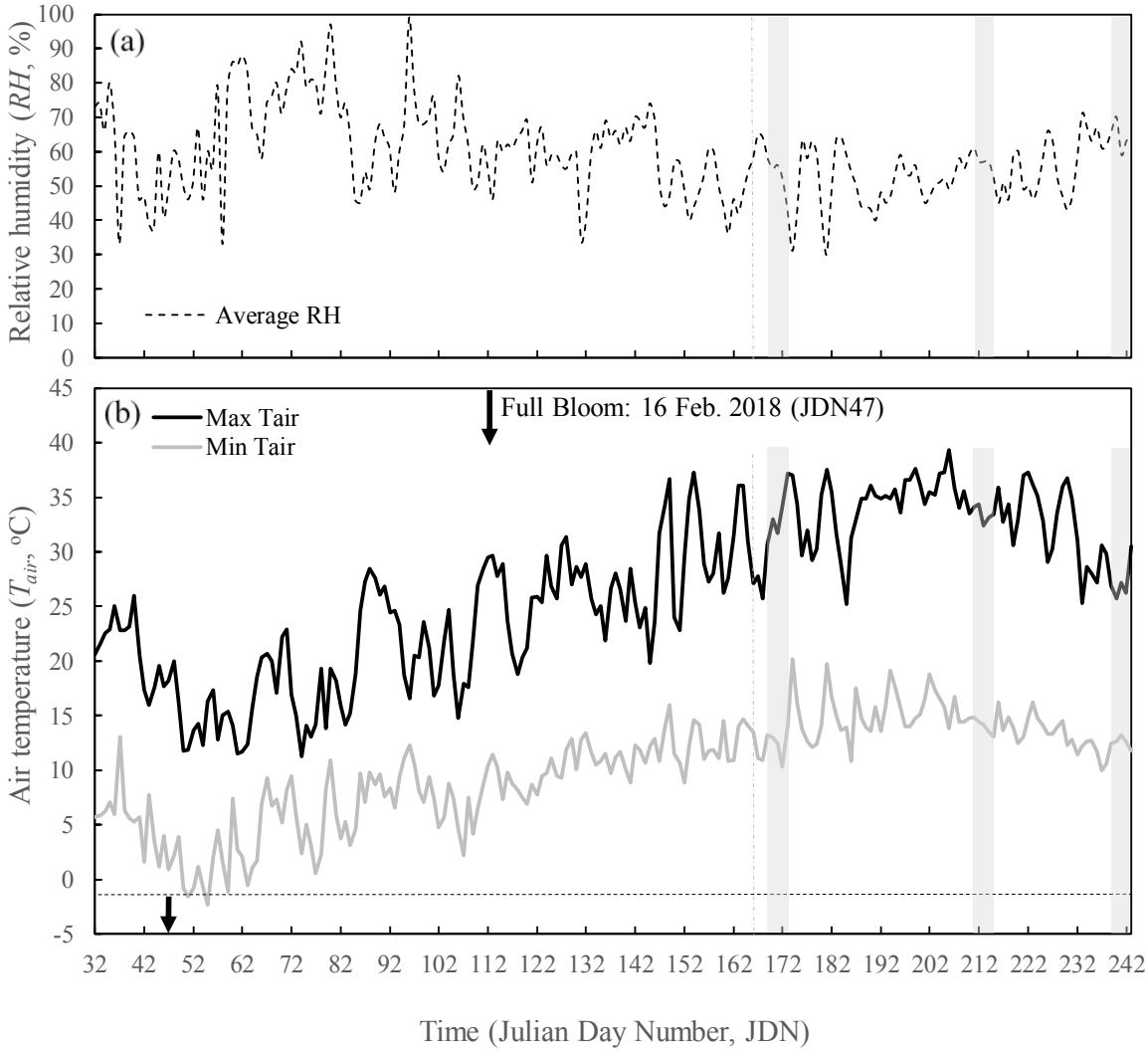

Fig. 3: *Time courses of daily average relative humidity (RH, %; a), daily minimum and maximum air temperatures (min T_{air} and max T_{air}, respectively; b) near the experimental site in Davis, California (USA, CIMIS weather station). The black arrow indicates the date of full bloom. The grey boxes or the vertical dot-dashed grey line indicate the measurement periods.*

In 2018, full bloom took place around 16 February 2018 just before a period of freezing (from JDN 50 to JDN 63). After that period of freezing, the minimum and maximum air temperatures increased: the maximum temperature of 39.3 °C was reached on JDN 206. The average daily minimum and maximum air temperatures during the experimental period (from JDN 166 to JDN 243) were 14.1 ± 2.1 °C (n = 78) and 32.9 ± 3.5 °C (n = 78), respectively (mean ± standard deviation). The average

relative humidity was 54.1 ± 8.5 % (from JDN 166 to JDN 243, n=78). The daily maximum air temperature was above 37.5 °C between JDN 199 and 206. From JDN 166 to JDN 243, the difference between the daily high and low temperatures was 18.8 ± 2.9 °C (n = 78) and the difference between the daily high and low relative humidity was 51.8 ± 9.1 % (n = 78). After JDN 216, the daily maximum and minimum air temperatures began to decrease. Figure 2 shows the values and the range of the air temperature and relative humidity recorded near the leaves (microclimate), during each of the measurement periods. The air temperatures varied from 20.7 ^{o}C to 38.4 ^{o}C. The relative humidity varied from 26.8% to 61.2%.

3.2 Effect of the light conditions and the side of the leaf on T_{wet} and T_{dry}

Figure 4 illustrates the effect of the light conditions and the side of the leaf on T_{dry} and T_{wet} for *P. dulcis*. At each date of measurement, no significant effect ($p < 0.05$) of the side of the leaf (upper or lower) was observed for T_{dry} and T_{wet}. Thus, the same model can be used for either side of the leaf to simulate the thermal temperature of non-transpiring (T_{dry}) or wet (T_{wet}) reference leaves. As expected, there was a significant effect of the light (sun and shade) on T_{dry} and T_{wet} ($p < 0.0001$, ANOVA, n = 12). In sunny conditions, T_{dry} and T_{wet} reached about 34.3 ^{o}C and 20.1 ^{o}C on average across all samples, respectively. In shady condition, T_{dry} and T_{wet} reached about 23.1 ^{o}C and 14.7 ^{o}C on average, respectively.

3.3 Comparison of the relationship between T_{dry}, T_{wet}, T_{ref}, and T_{air}

Figure 5 compares the relationships between T_{dry}, T_{wet} and T_{air}, and between T_{dry}, T_{wet} and T_{ref}. The relationship between T_{dry} and T_{ref} was nearly linear, with linear and quadratic regression models both providing an R^2_{adj} value greater than 0.84 for the paper colors considered. Similarly, the relationship between T_{wet} and T_{ref} was nearly linear, where the linear model gave an $R^2_{adj} > 0.71$, and the quadratic model gave $R^2_{adj} > 0.72$ (Table 2 and 3, Sun/Shade models). Prediction of T_{dry} and T_{wet} based on T_{ref} was much better than basing the model on T_{air}. Linear and quadratic models of T_{dry} based on T_{air} both yielded an R^2_{adj} of 0.32, and linear and quadratic models of T_{wet} based on T_{air} yielded an R^2_{adj} of 0.28 and 0.30, respectively. Fig. 5g shows that the line $T_{dry} = T_{air} + 5^{o}$C (estimation of T_{dry} with a constant offset use by Cohen *et al.*, 2005) over-estimates T_{dry} in shaded conditions, and gives high variability given that a single value of T_{air} corresponds to many different values of T_{dry}.

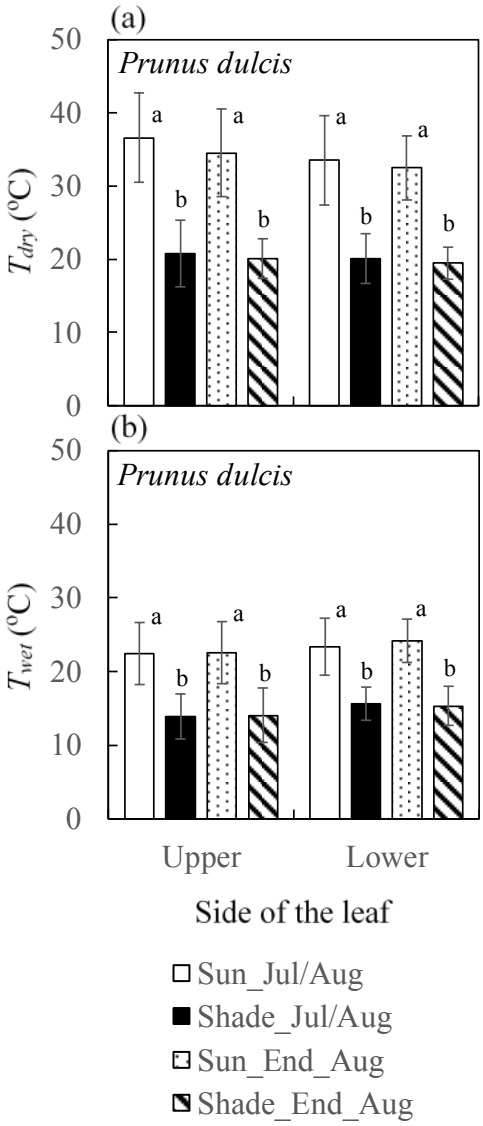

Fig. 4: *Effect of light conditions (sun or shade) and the side of the leaf (upper or lower) on the thermal temperature of non-transpiring (T_{dry}; a) or well-watered (T_{wet}; b) leaves for Prunus dulcis during summer 2018. Results are separated by measurement period, which occurred at the end of July/beginning of August (Jul/Aug) or at the end of August (End_Aug). Bar heights are average values ± SD (n = 12). Significant differences are denoted by letters above bars (ANOVA, Tukey test).*

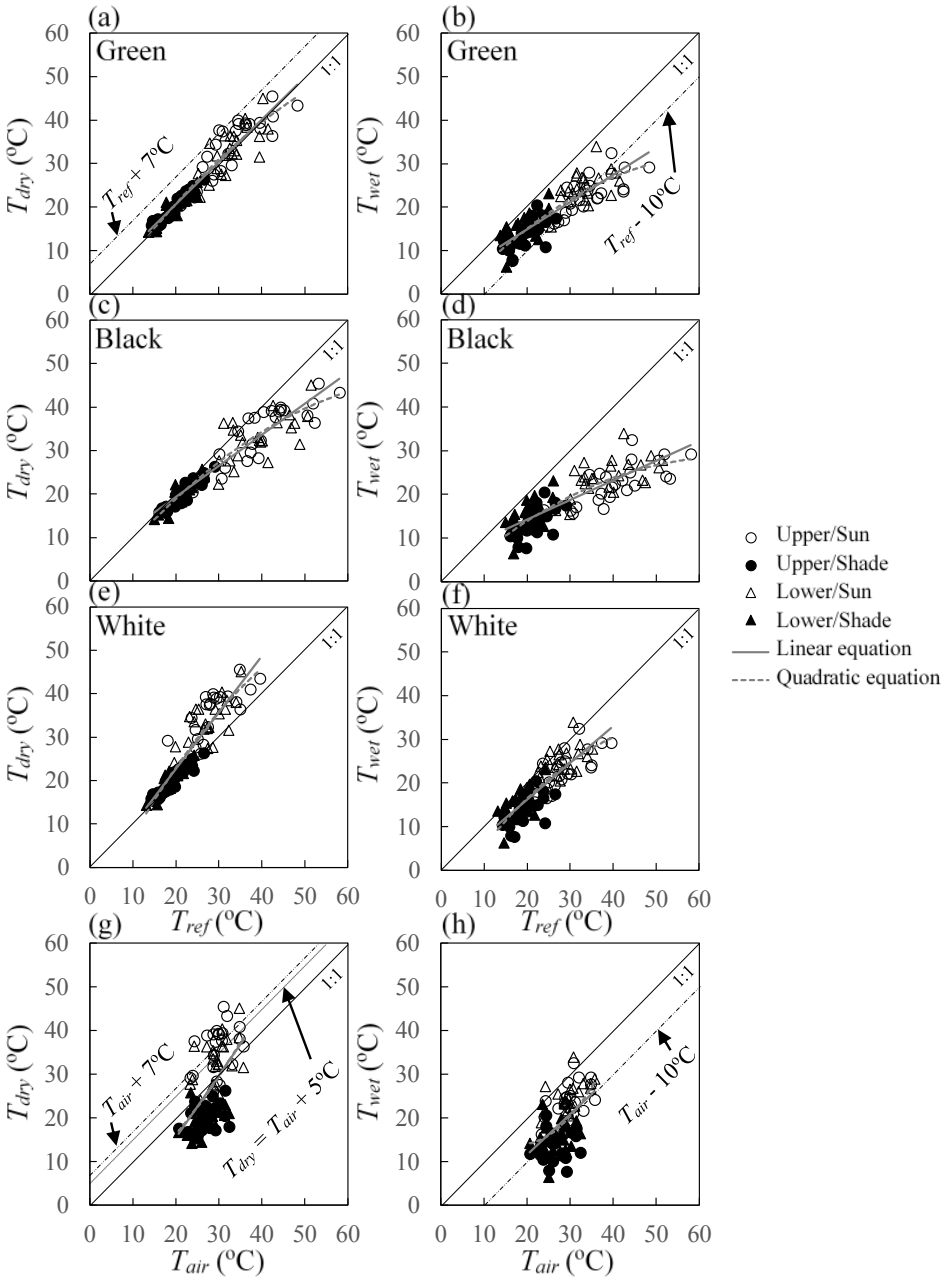

Fig. 5: *Relationship between T_{dry} (a, c, e) or T_{wet} (b, d, f) and T_{ref} (temperature of green (a and b), black (c and d) and white (e and f) reference paper) for the upper and lower sides of the leaf, in sunlit and shaded conditions. Relationship between T_{dry} (g) or T_{wet} (h) and T_{air} (measured near the leaf with the thermo-hygrometer probe) for the upper and lower sides of the leaf, in sunlit and shaded conditions. Only the data employed in the calibration step of the models were used in these figures. For reference, curves are shown for $T_{dry} = T_{air} + 5$ ºC (thin dotted line) representing the constant temperature offset approach (Cohen et al., 2005; g), $T_{air} + 7$ °C (g), $T_{air} - 10$ °C (h) representing the upper and lower thresholds according to the image processing of Meron (2010) (thin long dashed double dotted line), $T_{ref} + 7$ °C (a) and $T_{ref} - 10$°C (b) (thin long dashed double dotted line).*

3.4 Choice of the reference surface

The results of the covariance analysis used to study the effect of light conditions, side of the leaf, and thermal temperature of the reference surface are shown in Table 1. These results allow for a determination of whether one model can be used for both light conditions in the prediction of T_{dry} or T_{wet}. For T_{dry} and T_{wet}, no significant interaction ($p > 0.05$) between input variables was found between the factors. Thus, the slopes of the models are homogeneous. For green and white reference surfaces, a main significant effect ($p < 0.001$) was found with the 'thermal T °C of the reference surface' only. Thus, there is no difference in the *y*-intercept. As a result, only this variable was used in formulating the model, and the same model was proposed for both light conditions. For the black reference surface, main effects were found for 'light' and 'thermal T °C of the reference' factors. Thus, the *y*-intercepts are different between shady and sunny conditions and two models were studied: one for sunny conditions

Table 1: *p*-values of analysis of covariance and main interactions between factors (ANCOVA, n = 12) for the effect of light conditions (sun or shade), side of the leaf (upper or lower), and the thermal temperature of the reference surface. Significant values ($p < 0.05$) are underlined.

	T_{dry}			T_{wet}		
	Color of the reference			Color of the reference		
Effects and interactions	Green	Black	White	Green	Black	White
Thermal T°C of the reference surface [T_{ref}]	**<0.001**	**<0.001**	**<0.001**	**<0.001**	**<0.001**	**<0.001**
Light	0.392	**0.015**	0.137	0.307	**0.049**	0.245
Side of the leaf	0.883	0.469	0.919	0.411	0.240	0.479
[T_{ref}] × Light	0.907	0.052	0.903	0.427	0.080	0.754
[T_{ref}] × Side of the leaf	0.926	0.669	0.940	0.810	0.695	0.990
Light × Side of the leaf	0.701	0.455	0.936	0.944	0.750	0.904
[T_{ref}] × Light × Side of the leaf	0.806	0.528	0.759	0.891	0.869	0.867

Table 2: *Evaluation of the performance of linear and non-linear models for T_{dry} under sunlit and shaded conditions, which were based on different reference surface types. The data were divided into subsets either for model fitting (n = 96) or model validation (n = 32). The chosen model is indicated* ***in bold****.*

	Linear model ($T_{dry} = a[T_{ref}] + b$)					*Non-linear model ($T_{dry} = a[T_{ref}]^2 + b[T_{ref}] + c$)*				
	Color of the reference surface					Color of the reference surface				
	Green	Black			White	Green	Black			White
	Sun/Shade	Sun	Shade	Sun/Shade	Sun/Shade	Sun/Shade	Sun	Shade	Sun/Shade	Sun/Shade
Name of model	***Model 1***	*Model 2*	*Model 3*	*Model 4*	*Model 5*	*Model 6*	*Model 7*	*Model 8*	*Model 9*	*Model 10*
Description of the T_{dry} models										
a	**0.9717**	0.6039	0.8500	0.7168	1.2989	-0.0083	-0.0100	-0.0077	-0.0077	-0.0143
b	**1.2213**	9.6935	1.8533	4.9137	-3.2883	1.4391	1.4140	1.1811	1.2309	2.0028
c	**-**	-	-	-	-	-4.7355	-6.1970	-1.6036	-2.6380	-11.3929
Fitting (three trees, n=96)										
R^2_{adj}	**0.9009**	0.5972	0.8196	0.8843	0.8389	0.9046	0.6023	0.8167	0.8938	0.8420
RMSE										
Sunny conditions	**3.5550**	3.7214	-	3.8300	4.3015	3.3908	3.6583	-	3.6609	4.0804
Shady conditions	**1.2291**	-	1.2586	1.3568	2.1212	1.4054	-	1.2551	1.2661	2.3801
All (sunny/shady conditions)	**2.6598**	-	-	2.8731	3.3913	2.5954	-	-	2.7391	3.3402
d										
Sunny conditions	**0.9591**	0.9539	-	0.9525	0.9379	0.9620	0.9553	-	0.9554	0.9428
Shady conditions	**0.9933**	-	0.9932	0.9916	0.9789	0.9916	-	0.9932	0.9931	0.9746
All (sunny/shady conditions)	**0.9736**	-	-	0.9687	0.9550	0.9750	-	-	0.9719	0.9566
Validation (one tree, n=32)										
R^2_{adj}	**0.9007**	0.6776	0.9022	0.8836	0.9089	0.9060	0.6620	0.9046	0.8700	0.9014
$RMSE_P$										
Sunny conditions	**3.5391**	4.0726	-	4.2507	3.1099	3.5322	4.2138	-	4.1911	3.2075
Shady conditions	**0.9608**	-	1.2009	1.4396	1.7643	0.9531	-	1.2134	1.1718	1.9065
All (sunny/shady conditions)	**2.5931**	-	-	2.8624	2.5283	2.5870	-	-	3.0772	2.6385
d_P										
Sunny conditions	**0.9574**	0.9425	-	0.9512	0.9655	0.9566	0.9389	-	0.9398	0.9627
Shady conditions	**0.9951**	-	0.9926	0.9886	0.9834	0.9954	-	0.9924	0.9930	0.9817
All (sunny/shady conditions)	**0.9722**	-	-	0.9655	0.9727	0.9725	-	-	0.9613	0.9706

The global goodness-of-fit of the model was evaluated by three statistics: the coefficient of determination adjusted, R^2_{adj}; root mean squared error, RMSE; and the Willmott index of agreement, d. The predictive capacity was evaluated with an independent data sets using the same three indices: R^2_{adj}, d_P, $RMSE_P$ (root mean squared error of prediction).

and one for shady conditions. However, we have also proposed a single model for the both light conditions with the black reference surface to verify if a single model is adequate.

3.5 Calibration and validation of the model for T_{wet} and T_{dry}

Table 2 presents and compares five linear models and five quadratic models, the simplest non-linear models, without interaction, used to predict T_{dry} for *P. dulcis* according to the three reference surfaces. The models that use the green reference surface temperature are the best models for T_{dry} (linear and quadratic models, Table 2). Furthermore, the three error metrics showed only a very slight difference between the linear model (R^2_{adj} = 0.9009, d = 0.9736, RMSE = 2.6598) and the quadratic model (R^2_{adj} = 0.9046, d = 0.9750, RMSE = 2.5954). Thus, we have chosen to continue our study with the linear model n°1 (the simplest model), that uses the green reference surface as the independent variable:

$$T_{dry} = 0.9717 \times [T_{refgreen}] + 1.2213, \quad (9)$$

where $T_{refgreen}$ is the thermal temperature of the green paper reference surface (°C).

For *P. dulcis*, the linear model explained a high percentage of the variance (R^2_{adj} = 0.9009) with a highly significant effect of $T_{refgreen}$ ($p < 0.0001$). The RMSE and d were 2.66 °C and 0.97 (respectively) over values ranging from 14 °C to 48 °C (Fig. 6a, Table 2). The $RMSE_P$ and d_P were similar at 2.59 °C and 0.97 (respectively) over values ranging from 13 °C to 44 °C, showing good predictive performance (Fig.6b, Table 2).

Table 3 presents and compares five linear models and five quadratic models, the simplest non-linear models, without interaction, used to predict T_{wet} according to three reference surfaces (green, black and white) for *P. dulcis*. The models that use the green reference surface temperature are also the best models for T_{wet} (linear and quadratic models, Table 3). The three error metrics showed only a very slight difference between the linear model (R^2_{adj} = 0.7609,

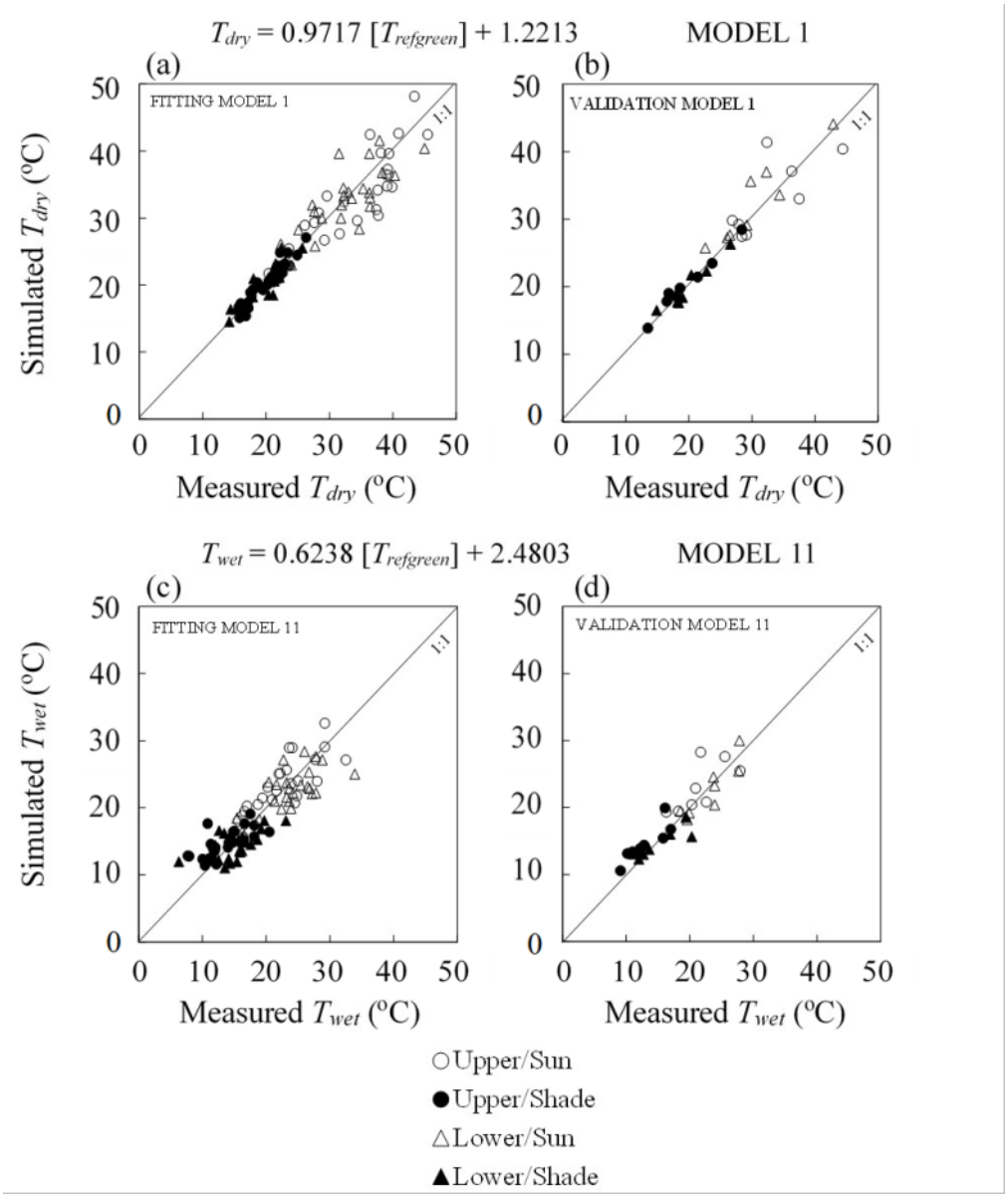

Fig. 6: *Comparison between the actual and modelled thermal temperature of non-transpiring (T_{dry}; a and b) or wet (T_{wet}; c and d) leaves for Prunus dulcis. The models (Eqns. 9 and 10) included one independent variable: the thermal temperature of a green reference surface ($T_{refgreen}$) placed within the thermal image. Panes a and c are based on the "fitting" data subset (n = 96); b and d are based on the "validation" data subset (n = 32).*

Table 3: *Evaluation of the performance of linear and non-linear models for T_{wet} under sunlit and shaded conditions, which were based on different reference surface types. The data were divided into subsets either for model fitting (n = 96) or model validation (n = 32). The chosen model is indicated* ***in bold****.*

	Linear model ($T_{wet} = a[T_{ref}] + b$)					*Non-linear model ($T_{wet} = a[T_{ref}]^2 + b[T_{ref}] + c$)*				
	Color of the reference surface					Color of the reference surface				
	Green	Black			White	Green	Black			White
	Sun/Shade	Sun	Shade	Sun/Shade	Sun/Shade	Sun/Shade	Sun	Shade	Sun/Shade	Sun/Shade
Name of the model	***Model 11***	*Model 12*	*Model 13*	*Model 14*	*Model 15*	*Model 16*	*Model 17*	*Model 18*	*Model 19*	*Model 20*
Description of the T_{wet} models										
a	**0.6238**	0.3562	0.5634	0.4495	0.8391	-0.0085	-0.0101	-0.0110	-0.0068	-0.0128
b	**2.4803**	9.1239	2.5669	5.1749	-0.5363	1.1006	1.1797	1.0344	0.9022	1.4689
c	**-**	-	-	-	-	-3.5969	-7.0312	-2.3509	-1.4744	-7.7882
Fitting (three trees, n=96)										
R^2_{adj}	**0.7609**	0.3831	0.2736	0.7122	0.7175	0.7686	0.3966	0.2593	0.7260	0.7225
RMSE										
Sunny conditions	**3.1172**	3.3588	-	3.4411	3.3277	2.9809	3.2857	-	3.2941	3.1501
Shady conditions	**2.6274**	-	2.8250	2.8573	2.9258	2.6512	-	2.8217	2.8264	3.0266
All (sunny/shady conditions)	**2.8827**	-	-	3.1627	3.1332	2.8209	-	-	3.0692	3.0890
d										
Sunny conditions	**0.9255**	0.9085	-	0.9064	0.9131	0.9298	0.9138	-	0.9116	0.9199
Shady conditions	**0.9322**	-	0.9225	0.9155	0.9114	0.9348	-	0.9226	0.9232	0.9106
All (sunny/shady conditions)	**0.9284**	-	-	0.9103	0.9124	0.9321	-	-	0.9169	0.9157
Validation (one tree, n=32)										
R^2_{adj}	**0.8304**	0.2708	0.4592	0.7491	0.7845	0.8544	0.2897	0.5071	0.7700	0.7957
$RMSE_P$										
Sunny conditions	**2.4707**	3.0427	-	3.0785	2.5379	2.2762	3.0870	-	3.0430	2.4389
Shady conditions	**2.0249**	-	2.3226	2.4113	2.5845	1.9171	-	2.2167	2.2587	2.5770
All (sunny/shady conditions)	**2.2588**	-	-	2.7651	2.5613	2.1043	-	-	2.6797	2.5089
d_P										
Sunny conditions	**0.9506**	0.9208	-	0.9194	0.9454	0.9568	0.9216	-	0.9218	0.9488
Shady conditions	**0.9547**	-	0.9419	0.9315	0.9262	0.9625	-	0.9468	0.9460	0.9316
All (sunny/shady conditions)	**0.9524**	-	-	0.9245	0.9371	0.9594	-	-	0.9325	0.9410

The global goodness-of-fit of the model was evaluated by three statistics: the coefficient of determination adjusted, R^2_{adj}; root mean squared error, RMSE; and the Willmott index of agreement, d. The predictive capacity was evaluated with an independent data sets using the same three indices: R^2_{adj}, d_P, $RMSE_P$ (root mean squared error of prediction).

Table 4: *Validation and generalization test of the chosen models to predict T_{dry} (model n°1) and T_{wet} (model n°11) on the leaves of five other hypostomatous species trees under sunlit and shaded conditions (n = 102; Nerium oleander, Olea europaea, Prunus persica, Quercus sp., Ulmus hybrid 'frontier').*

	Validation with other species						
	R^2_{adj}	$RMSE_P$			d_P		
$[T_{refgreen}]$ = Thermal T°C of green reference surface		*Sun*	*Shade*	Sun/Shade	*Sun*	*Shade*	Sun/Shade
Model 1 (Model of T_{dry})							
$T_{dry} = 0.9717[T_{refgreen}] + 1.2213$							
Global (n=102)	0.8843	3.2781	1.3449	2.5229	0.9546	0.9808	0.9618
Nerium oleander ($n=8_{shade};10_{sun}$)	0.6584	5.2463	0.8479	3.9510	0.8460	0.9906	0.8830
Olea europaea ($n=9_{shade}; 9_{sun}$)	0.8057	3.2028	0.8440	2.3421	0.8574	0.9942	0.9436
Prunus persica ($n=12_{shade}; 12_{sun}$)	0.9423	2.8258	1.8202	2.3768	0.9841	0.9786	0.9828
Quercus sp. ($n=9_{shade}; 9_{sun}$)	0.8934	1.5949	1.5238	1.5598	0.9663	0.9627	0.9646
Ulmus hybrid 'frontier'($n=12_{shade}; 12_{sun}$)	0.8840	2.4580	1.2117	1.9378	0.9770	0.9688	0.9758
Model 11 (Model of T_{wet})							
$T_{wet} = 0.6238[T_{refgreen}] + 2.4803$							
Global (n=102)	0.7568	2.5519	2.2495	2.4084	0.9391	0.8961	0.9260
Nerium oleander ($n=8_{shade};10_{sun}$)	0.6603	2.4547	2.1801	2.3366	0.9111	0.8085	0.8878
Olea europaea ($n=9_{shade}; 9_{sun}$)	0.7660	1.2694	1.3959	1.3342	0.9409	0.9609	0.9538
Prunus persica ($n=12_{shade}; 12_{sun}$)	0.9209	2.9286	1.4728	2.3179	0.9662	0.9716	0.9674
Quercus sp. ($n=9_{shade}; 9_{sun}$)	0.6672	3.0692	2.5347	2.8147	0.6813	0.8785	0.8827
Ulmus hybrid 'frontier' ($n=12_{shade}; 12_{sun}$)	0.7061	2.5194	3.0768	3.0802	0.9427	0.7136	0.8901

d = 0.9284, RMSE = 2.8827) and the quadratic model (R^2_{adj} = 0.7686, d = 0.9321, RMSE = 2.8209). Likewise, we have chosen to continue our study with the linear model n°11 (the simplest model), that uses the green reference surface as the independent variable:

$$T_{wet} = 0.6238 \times [T_{refgreen}] + 2.4803. \quad (10)$$

For *P. dulcis*, the linear model explained a large percentage of the variance (R^2_{adj} = 0.7609) with a highly significant effect of [$T_{refgreen}$] ($p < 0.0001$). The RMSE and d were acceptable at 2.88 °C and 0.93 (respectively) over values ranging from 11 °C to 33 °C (Fig. 6c, Table 3). The $RMSE_P$ and d_P were also acceptable at 2.26 °C and 0.95 (respectively) over values ranging from 10 °C to 30 °C, showing the applicability for data independent of that used to build it (Fig. 6d, Table 3). For all studied models, the fit of the models of T_{dry} and T_{wet} was better for the shady conditions than the sunny conditions (Table 2 and Table 3).

3.6 Generalization to other species

We tested the previous models (model n°1 and model n°11) on additional data to evaluate the generalization of the models to others hypostomatous species and at other nearby locations. Figure 7 shows the relationship between measured and modeled T_{dry} and T_{wet} for *N. oleander*, *O. europaea*, *P. persica*, *Q. sp*. and *U. hybrid* 'frontier'. For model n°1 (model of T_{dry}), the overall of $RMSE_P$ and d_P were 2.52 °C and 0.96, respectively, over values ranging from 12 °C and 43 °C (Table 4), which was very close to the 2.59 °C $RMSE_P$ value found for *P. dulcis* (Table 2). For model n°11 (model of T_{wet}), the overall $RMSE_P$ and d_P were 2.41 °C and 0.93 (respectively) over values ranging from 9 °C to 29 °C (Table 4), which was close to the 2.26 °C $RMSE_P$ value found for *P. dulcis* (Table 3). These results showed the generalization of the linear models to other species and other locations. As mentioned previously, the fit of the models is better for the shady conditions than the sunny conditions. Among the other studies species, *P. persica* showed the best R^2_{adj} and d_P (R^2_{adj} = 0.9423 and 0.9209; d_P = 0.9828 and 0.9674, for T_{dry} and T_{wet}, respectively).

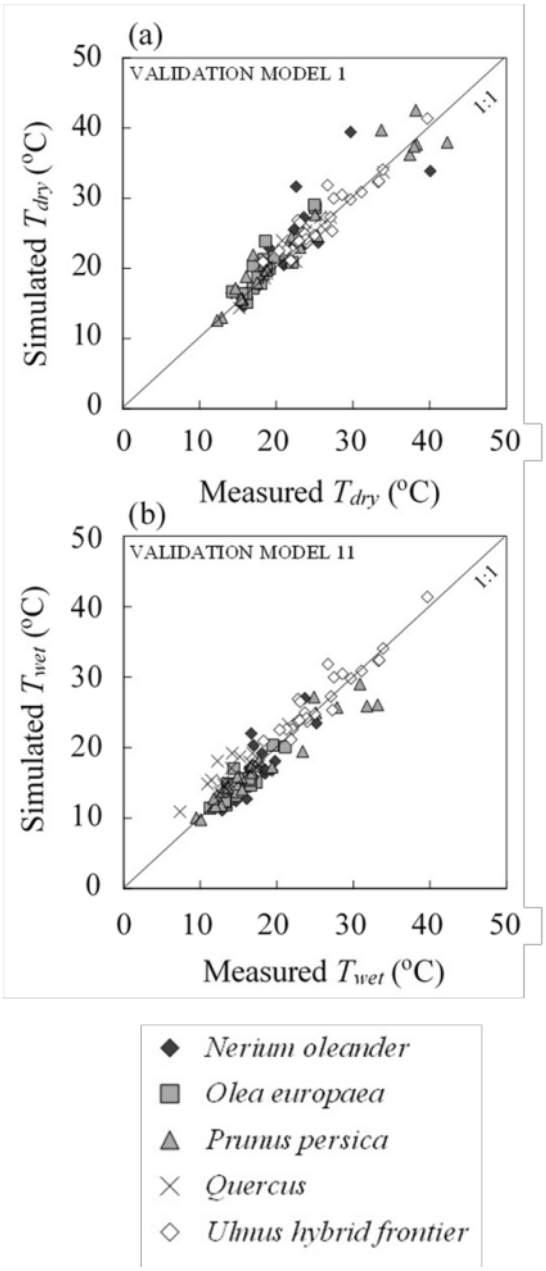

Fig. 7: *Comparison between the actual and modelled thermal temperature of non-transpiring (T_{dry}; a) and well-watered (T_{wet}; b) leaves for hypostomatous species Nerium oleander, Olea europaea, Prunus persica, Quercus sp., Ulmus hybrid 'frontier'. The models (Eqns. 9 and 10) were parameterized based on data from Prunus dulcis and included one independent variable: the thermal temperature of a green reference surface ($T_{refgreen}$) placed within the thermal image.*

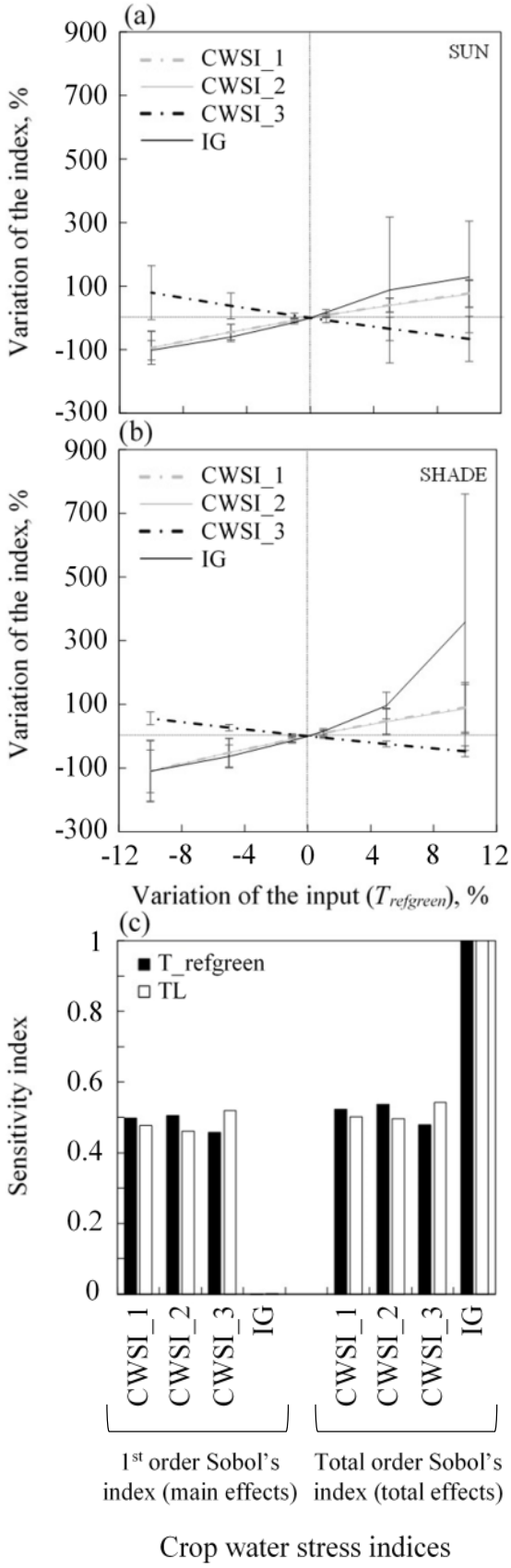

Fig. 8: *Sensitivity analysis of the CWSIs in the sun (a) and in the shade (b). Percentage variation of the CWSI (average ± SD, n = 12) due to a ± 10% variation of the temperature of the green reference ($T_{refgreen}$) with T_L held constant for four CWSIs ($CWSI_1 = (T_{dry} - T_L) / T_{dry}$, $CWSI_2 = (T_L - T_{dry}) / (T_{wet} - T_{dry})$, $CWSI_3 = (T_L - T_{wet}) / T_{wet}$, $I_G = (T_{dry} - T_L) / (T_L - T_{wet})$). The x- and y-axis crossing at 0 are indicated with dashed thin lines. (c) Sobol sensitivity indices (first and total orders; with the formulas of Martinez (2011)) of the two parameters $T_{refgreen}$ (range for the sensitivity analysis: [20 – 45] °C) and T_L (range for the sensitivity analysis: [20 – 45] °C) used in the calculation of the four CWSIs ($CWSI_1$, $CWSI_2$, $CWSI_3$ and I_G).*

3.7 Sensitivity analysis of four Crop Water Stress Indices (CWSIs)

Figures 8a (sunlit) and 8b (shaded) show the effect of varying the temperature of the green reference surface ($T_{refgreen}$) on four CWSIs with T_L fixed. Over the range of -10% to +10% and for the two light conditions, the four indices vary significantly ($p < 0.001$) (Fig. 8a and 8b). In the sun, I_G was the index most influenced by a variation of +10% of the input $T_{refgreen}$ (+129%) and $CWSI_3$ the least influenced index (-66%, $p < 0.012$). For a variation of -10% of the input $T_{refgreen}$, $CWSI_3$ was the least influenced index (+79%, $p < 0.001$) as opposed to -94%, -94%, -102% for $CWSI_1$, $CWSI_2$, I_G, respectively (Fig. 8a). In the shade, I_G was also the index most influenced by a variation of +10% of the input $T_{refgreen}$ (+358%; $p < 0.047$) and $CWSI_3$ the least influenced index (-47%; $p < 0.009$). For a variation of -10% of the input $T_{refgreen}$, $CWSI_3$ was the least influenced index (+56%; $p < 0.001$) as opposed to -110% for $CWSI_1$, $CWSI_2$ and I_G (no significative difference between these three CWSIs, $p > 0.89$; Fig. 8b).

Figure 8c shows the results of the Sobol sensitivity analysis (with the formulas of Martinez (2011)) for four CWSIs with variation of parameters $T_{refgreen}$ and T_L. Sobol's method determines the contribution of each input parameter ($T_{refgreen}$ and T_L) to overall output variance (first-order sensitivity index) and their interactions (total-order sensitivity index). For $CWSI_1$ and $CWSI_2$, the results indicate that $T_{refgreen}$ is the most important parameter, individually contributing to around 50% of both outputs (CWSI) and T_L contributing to around 48% and 46% of the output, respectively. In other words, most of the variation in these CWSIs was due to $T_{refgreen}$. For $CWSI_3$, the result indicates that T_L is the most important parameter, individually contributing to around 52% of the output (CWSI). In other words, most of the variation in this CWSI was due to T_L. On the other hand, $CWSI_3$ presents the biggest difference between the first-order sensitivity indices of $T_{refgreen}$ and T_L (46% and 52%, respectively). For $CWSI_1$, $CWSI_2$ and $CWSI_3$, both the first-order sensitivity indices and the total-order sensitivity indices have similar values, which indicates no significant second-order interaction between $T_{refgreen}$ and T_L. I_G, $T_{refgreen}$ and T_L have no main effects (first-order sensitivity index of $I_G << 0.05$ for both parameters). However, the values of the total-order sensitivity indices are close to 1 indicating that the variance of I_G was driven mainly by the second-order interaction between $T_{refgreen}$ and T_L (Fig. 8c). As illustrated graphically in Fig. 8c, the ratio between the sensitivity of CWSI to T_L and $T_{refgreen}$ is

largest for $CWSI_3$. This means that $CWSI_3$ is likely to be least sensitive (in a relative sense) to errors in the estimation of reference temperatures via $T_{refgreen}$.

4. DISCUSSION

4.1 Effect of the light conditions on T_{dry} and T_{wet}

Our results indicated a significant effect of the light conditions on T_{dry} and T_{wet}, and the fit of the model is better for the data recorded in the shade than in the sun, which is in agreement with previously reported results (Ansari and Loomis, 1959; Atkin *et al.*, 2000; Niesenbaum and Kluger, 2006). For example, Dhillon *et al.* (2014) found an analogous result for a multiple linear regression model for leaf temperature as a function of mid-day stem water potential and environmental variables, in which the R^2 was better for shaded leaves than for sunlit leaves. They suggested that the influence of factors such as sun angle and leaf orientation were stronger in the case of sunlit leaves, as PAR was found to be significant in all sunlit leaf models. Other previous studies also indicated that at a low irradiance (i.e., shade), the variance in temperature declines to low levels and at the high irradiance (i.e., full sun), the variance is amplified by decreasing irradiance within the canopy (Ngao *et al.*, 2017). More diffuse irradiance homogenizes the leaf temperatures because shaded leaves receive proportionally more radiative energy under those conditions (Woods *et al.*, 2017). That could explain the differences observed in the fit of the models in the sun and shade. Although light has a strong effect on the temperature of the well-watered and non-transpiring leaves (T_{dry} and T_{wet}), the model that relates the reference temperature to T_{dry} and T_{wet} is the same. This has important practical implications, particularly if the method is applied to a whole tree/plant that contains both sunlit and shaded leaves in one image.

4.2 Effect of the side of the leaf on T_{dry} and T_{wet}

Almond leaves are hypostomatous (Palasciano *et al.*, 2005), i.e., the stomata are mostly on the lower side of the leaf. Our results showed that the thermal temperature of the leaf is approximately the same on the both sides of the leaf for T_{dry} and T_{wet}. Pallas *et al.* (1967) found that in cotton plants (*Gossypiunt hirsutum* L.) differences in temperature between the upper and lower leaf surfaces could reach 2 ^{o}C, where the upper surface was warmer than the lower when the leaf was well-hydrated, and the converse was true under drought stress conditions. They also reported that the

temperature differences between the upper and lower surfaces were only significant under high light conditions. The authors attributed these differences to a combination of differential heating due to radiation, differential cooling due to radiation, and changes in leaf angle mediated by turgor changes. However, their results could also be explained by radiation error of the thermocouple which has been reported to cause similar magnitude errors (Bailey *et al*., 2016) combined with varying leaf angle that could change the nature of the radiation error. The ability to assume the same temperature for upper and lower faces of the leaf is potentially important for application of thermal imaging in whole-plants or -canopies because any given view of the vegetation may contain both upper and lower leaf surfaces. If, as our results suggest, differences in leaf temperature between upper and lower leaf faces are small, then this eliminates an additional variable that would need to be accounted for when processing the thermal images.

4.3 Model of T_{dry} and T_{wet} to increase ease-of-use

One goal of this work was to determine artificial reference surfaces that could be easily used (without any further measurement) to estimate T_{dry} and T_{wet}, and thus make the CWSI approach easier to apply in the field, particularly by growers. We developed simple models to predict T_{dry} and T_{wet} (during the growing season) based only on the temperature of a green paper reference surface ($T_{refgreen}$) under the same conditions as the leaf being examined. The proposed models are relatively simple in that they are linear equations with only $T_{refgreen}$ as the independent variable. The models were calibrated, validated and tested with data recorded under a wide range of air temperature and relative humidity conditions (Fig. 2). Although it was not possible to test the model for all possible environmental conditions, it was shown to perform well at three different times during the growing season and across six different species.

It is perhaps surprising the wet reference temperature can be estimated using the temperature of a dry piece of paper because it would seemingly lack the effect of evaporation. Poirier-Pocovi and Bailey (2020) showed that, when in sunlight, T_{wet} is only weakly dependent on relative humidity. As with T_{dry}, T_{wet} is driven primarily by air temperature and wind speed in direct sunlight. Since the green reference surface also includes these environmental factors, a model based on $T_{refgreen}$ is able to explain most of the variation in T_{wet}.

A common approach for estimating T_{dry} is to assume that T_{dry} is a constant offset above the air temperature (e.g., $T_{dry} = T_{air} + 5$ ºC; Cohen *et al.*, 2005). This approach presents several possible problems. Several environmental variables such as the light, the wind speed, or the relative humidity can influence the difference between the surface temperature of the leaf reference and the air temperature. Indeed, if the constant temperature offset approach is applied, Figures 5g show that the values of T_{dry} are over estimated in the shade. Also, high variability of T_{dry} was observed for the same value of T_{air}, which is not present for the models based on $T_{refgreen}$. Some studies such as Meron *et al.* (2010) in cotton or García-Tejero *et al.* (2012) in almond trees developed an empirical methodology for canopy temperature extraction using thermal images and air temperature. The proposed methodology was based on the separation of the canopy-related pixels in the thermal image from those of the soil and other objects by upper and lower thresholds to air temperature. Our results indicate that it would probably be better to use T_{ref} in this step of processing images. Indeed, if T_{air} is used in the upper and lower thresholds, a lot of interesting data would be deleted during the pixel filtering process (Fig. 5g, 5h); less data would be lost with T_{ref} (Fig. 5a, 5b).

Furthermore, by using temperature measurements from different instruments in the CWSI, systematic errors in the temperature measurements will not necessarily cancel such as absolute errors in the thermographic measurement. The method proposed in this work requires only slightly more effort to apply than the constant temperature offset method, but it also takes into account important environmental variables that influence T_{dry} and T_{wet}.

4.4 Performance of these new models in the estimation of four crop water stress indices for almond trees

Previous work does not exist in the literature regarding thorough analysis of the sensitivity of CWSIs to errors in estimation of T_{dry} and T_{wet} reference temperatures. Our new results suggest that I_G is the most sensitive index to the variation of input $T_{refgreen}$ (Fig. 8a, 8b) and the output value is influenced by the interaction between $T_{refgreen}$ and T_L (Fig. 8c). In the definition of this index, T_{dry} is only in the numerator and thus its influence is much more important. In the other indices, T_{dry} is present in the numerator and denominator of the equation ($CWSI_1$ and $CWSI_2$) or absent altogether ($CWSI_3$), which limits the ultimate influence of T_{dry} on the estimation of the

crop water stress index. The sensitivity to I_G was markedly different from the other three, because T_L is present in both the numerator and denominator, which means that its influence on the CWSI comes in through relative interactions with T_{wet} and T_{dry}. The sensitivity analysis showed that $CWSI_3$ was most sensitive to T_L out of $CWSI_1$, $CWSI_2$ and I_G. Its evolution seems to better reflect the changes of the leaf temperature. Since the estimation of reference surface temperatures will always incur some error in estimating CWSIs, we seek a CWSI that has maximum sensitivity to T_L (which is directly measured) and minimum sensitivity to the reference temperature (in our case estimated from $T_{refgreen}$). Thus, based on our sensitivity analysis, $CWSI_3$ appears most suitable because it has both of these characteristics. Additional experiments are necessary to verify if $CWSI_3$ can be used to estimate the water needs and manage the irrigation of the almond trees.

5. CONCLUSION

The present study proposes a methodology for modeling the reference temperatures T_{dry} and T_{wet} commonly used in CWSIs. It was determined that T_{dry} and T_{wet} could be related to the temperature of a green piece of paper using simple linear models. This approach was developed using almond trees and tested on other five other species. We also analyzed the sensitivity of these models in the estimation of four CWSIs, including a new CWSI, denoted as $CWSI_3$, based only on T_L and T_{wet}. A sensitivity analysis indicated that $CWSI_3$ appeared promising in that it had the highest sensitivity to T_L but had the lowest sensitivity to the temperature of the reference paper $T_{refgreen}$.

Our study is an initial step toward improving the accessibility and adoption of thermography-based irrigation management tools by growers by making them easier to use and less expensive. Additional work is needed to evaluate the performance of the new index $CWSI_3$ in estimating tree water status and associated irrigation needs, and to further evaluate the approach over seasonal time periods. There is potential to scale up the approach to the field level using airborne sensing platforms by placing a large green surface of paper in the orchard and using the new models of T_{dry} and T_{wet} to define the wet and dry leaf reference surface temperatures.

6. ACKNOWLEDGEMENTS

This work was supported by the Almond Board of California, and by USDA National Institute of Agriculture Hatch projects 1013396 (BNB) and CA-D-PLS-2247-H (AV).

7. References

Alchanatis, V., Cohen, Y., Cohen, S., Moller, M., Sprinstin, M., Meron, M., Tsipris, J., Saranga, Y., Sela, E., 2010. Evaluation of different approaches for estimating and mapping crop water status in cotton with thermal imaging. *Precis. Agric*. 11, 27-41. https://doi.org/10.1007/s11119-009-9111-7

Ansari, A.Q., Loomis, W.E., 1959. Leaf Temperatures. *Am. J. Bot.* 46(10), 713-717. https://doi.org/10.1002/j.1537-2197.1959.tb07076.x

Atkin, O.K., Evans, J.R., Ball, M.C., Lambers, H., Pons, T.L., 2000. Leaf respiration of snow gum in the light and dark. Interactions between temperature and irradiance. *Plant Physiol.* 122, 915-923. https://doi.org/10.1104/pp.122.3.915

Bailey, B.N., Stoll, R., and Pardyjak, E.R., Miller, N.E., 2016. A new three-dimensional energy balance model for complex plant canopy geometries: Model development and improved validation strategies. *Agr. Forest Meteorol*. 218-219, 146-160. https://doi.org/10.1016/j.agrformet.2015.11.021

Ballester, C., Castel, J., Jiménez-Bello, M.A., Castel, J.R., Intrigliolo, D.S., 2013. Thermographic measurement of canopy temperature is a useful tool for predicting water deficit effects on fruit weight in citrus trees. *Agr. Water Manage.* 122, 1-6. https://doi.org/10.1016/j.agwat.2013.02.005

Baudin, M., Boumhaout, K., Delage, T., Iooss, B., Martinez, J-M., 2016. Numerical stability of Sobol' indices estimation formula, Proceedings of the SAMO 2016 Conference, Reunion Island, France, December 2016

Bellvert, J., Marsal, J., Girona, J., Zarco-Tejada, P.J., 2015. Seasonal evolution of crop water stress index in grapevine varieties determined with high-resolution remote sensing thermal imagery. *Irrig. Sci.* 33, 81-93. https://doi.org/10.1007/s00271-014-0456-y

Campbell, G.S., Norman, J.M., 1998. An introduction to environmental biophysics. 2nd edition. New York: Springer. pp 286

Cohen, Y., Alchanatis, V., Meron, M., Saranga, Y., Tsipris, J., 2005. Estimation of leaf water potential by thermal imagery and spatial analysis. *J. Exp. Bot.* 56(417), 1843-1852. https://doi.org/10.1093/jxb/eri174

Cohen, Y., Alchanatis, V., Saranga, Y., Rosenberg, O., Sela, E., Bosak, A., 2017. Mapping water status based on aerial thermal imagery: comparison of methodologies for upscaling from a single leaf to commercial fields. *Precis. Agric*. 18, 801-822. https://doi.org/10.1007/s11119-016-9484-3

Costa, J.M., Grant, O.M., Chaves, M.M., 2013. Thermography to explore plant-environment interactions. *J. Exp. Bot.* 64, 3937-3949. https://doi.org/10.1093/jxb/ert029

Craparo, A.C.W., Steppe, K., Van Asten, P.J.A., Läderach, P., Jassogne, L.T.P., Grab, S.W., 2017. Application of thermography for monitoring stomatal conductance of *Coffea Arabica* under different shading systems. *Sci. Total Environ*. 609, 755-763. https://doi.org/10.1016/j.scitotenv.2017.07.158

Dhillon, R., Udompetaikul, V., Rojo, F., Roach, J., Upadhyaya, S., Slaughter, D., Lampinen, B., Shackel, K., 2014. Detection of plant water stress using leaf temperature and microclimatic measurements in almond, walnut, and grape crops. *ASABE*. 57(1), 297-304. https://doi.org/10.13031/trans.57.10319

Dinçer, C., Topuz, A., 2015. Inactivation of *Escherichia coli* and quality changes in black mulberry juice under pulsed sonication and continuous thermosonication treatments. *J. Food Process. Pres.* 39(6), 1744-1753. https://doi.org/10.1111/jfpp.12406

Engqvist, L., 2005. The mistreatment of covariate interaction terms in linear model analyses of behavioural and evolutionary ecology studies. *Anim. Behav.* 70, 967-971. https://doi.org/10.1016/j.anbehav.2005.01.016

FLIR®, 2017. Thermographic measurement techniques. *In* User's manual FLIR ETS3xx series (pp. 43-47). https://www.flir.com/globalassets/imported-assets/document/flir-ets320-user-manual.pdf (accessed 27 June 2018).

García-Tejero, I., Durán-Zuazo, V.H., Arriaga, J., Hernández, A., Vélez, L.M., Muriel-Fernández, J.L., 2012. Approach to assess infrared thermal imaging of almond trees under water-stress conditions. *Fruits*. 67, 463-474. https://doi.org/10.1051/fruits/2012040

García-Tejero, I., Costa, J.M., Egipto, R., Durán-Zuazo, V.H., Lima, R.S.N., Lopes, C., Chaves, M.M., 2016. Thermal data to monitor crop-water status in irrigated Mediterranean viticulture. *Agr. Water Manage.* 176, 80-90. https://doi.org/10.1016/j.agwat.2016.05.008

García-Tejero, I.F., Hernández, A., Padilla-Díaz, C.M., Diaz-Espejo, A., Fernández, J.E., 2017. Assessing plant water status in a hedgerow olive orchard from thermography at plant level. *Agr. Water Manage*. 188, 50-60. https://doi.org/10.1016/j.agwat.2017.04.004

Gerhards, M., Rock, G., Schlerf, M., Udelhoven, T., 2016. Water stress detection in potato plants using leaf temperature, emissivity, and reflectance. *Int. J. Appl. Earth Obs.* 53, 27-39. https://doi.org/10.1016/j.jag.2016.08.004

Grant, O.M., Tronina, Ł., Jones, H.G., Chaves, M.M., 2007. Exploring thermal imaging variables for the detection of stress responses in grapevine under different irrigation regimes. *J. Exp. Bot.* 58(4), 815-825. https://doi.org/10.1093/jxb/erl153

Gutiérrez, S., Diago, M.P., Fernández-Novales, J., Tardaguila, J., 2018. Vineyard water status assessment using on-the-go thermal imaging and machine learning. *PLoS ONE*. 13(2), e0192037. https://doi.org/10.1371/journal.pone.0192037

Hill, T., Lewicki, P., 2007. Statistics methods and applications. StatSoft, Tulsa, OK, 70 pp.

Hopkins, W.G., 2003. Physiologie végétale, Bruxelles, De Boeck Supérieur, pp 532

Idso, S.B., 1982. Non-water stressed baselines: a key to measuring and interpreting plant water stress. *Agr. Meteorol.* 27, 59-70. https://doi.org/10.1016/0002-1571(82)90020-6

Janssen, P.H.M., Heuberger, P.S.C., 1995. Calibration of process-oriented models. *Ecol. Model*. 83, 55-66. https://doi.org/10.1016/0304-3800(95)00084-9

Jones, H.G., 1999. Use of infrared thermometry for estimation of stomatal conductance in irrigation scheduling. *Agr. Forest Meteorol*. 95, 135-149. https://doi.org/10.1016/S0168-1923(99)00030-1

Jones, H.G., Stoll, M., Santos, T., De Sousa, C., Chaves, M.M., Grant, O.M., 2002. Use of infrared thermography for monitoring stomatal closure in the field: application to grapevine. *J.Exp. Bot.* 53(378), 2249-2260. https://doi.org/10.1093/jxb/erf083

Maes, W.H., Baert, A., Huete, A.R., Minchin, P.E.H., Snelgar, W.P., Steppe, K., 2016. A new wet reference target method for continuous infrared thermography of vegetations. *Agr. Forest Meteorol.* 226–227, 119-131. https://doi.org/10.1016/j.agrformet.2016.05.021

Martinez, J-M., 2011. Analyse de sensibilité globale par décomposition de la variance, Presentation in the meeting of GdR Ondes and GdR MASCOT-NUM, January 13th, 2011, Institut Henri Poincaré, Paris, France.

Meron, M., Tsipris, J., Orlov, V., Alchanatis, V., Cohen, Y., 2010. Crop water stress mapping for site specific irrigation by thermal imagery and artificial reference surfaces. *Precis. Agric.* 11, 148-162. https://doi.org/10.1007/s11119-009-9153-x

Möller, M., Alchanatis, V., Cohen, Y., Meron, M., Tsipris, J., Naor, A., Ostrovsky, V., Sprintsin, M., Cohen, S., 2007. Use of thermal and visible imagery for estimating crop water status of irrigated grapevine. *J. Exp. Bot.* 58, 827-838. https://doi.org/10.1093/jxb/erl115

Niesenbaum, R.A., Kluger, E.C., 2006. When studying the effects of light on herbivory, should one consider temperature? The case of *Epimecis hortaria* F. (Lepidoptera: Geometridae) feeding on *Lindera benzoin* L. (Lauraceae), *Environ. Entomol.* 35(3), 600–606. https://doi.org/10.1603/0046-225X-35.3.600

Ngao, J., Adam, B., Saudreau, M., 2017. Intra-crown spatial variability of leaf temperature and stomatal conductance enhanced by drought in apple tree as assessed by the RATP model. *Agr.Forest Meteorol.* 237–238, 340–354. https://doi.org/10.1016/j.agrformet.2017.02.036

Palasciano, M., Camposeo, S., Godini, A., 2005. Stomatal size and frequency in wild (*A. webbii*) and cultivated (*A. communis*) almonds. In: Oliveira M.M. (ed.), Cordeiro V. (ed.). XIII GREMPA Meeting on Almonds and Pistachios. Zaragoza: CIHEAM, 2005. p. 305-310 (Options Méditerranéennes : Série A. Séminaires Méditerranéens ; n. 63)

Pallas, J.E. JR., Michel, B.E., Harris, D.G., 1967. Photosynthesis, transpiration, leaf temperature, and stomatal activity of cotton plants under varying water potentials. *Plant Physiol.* 42, 76-88. https://doi.org/10.1104/pp.42.1.76

Pianosi, F., Beven, K., Freer, J., Hall, J.W., Rougier, J., Stephenson, D.B., Wagener, T., 2016. Sensitivity analysis of environmental models: A systematic review with practical workflow. *Environ. Modell. Softw.* 79, 214-232. https://doi.org/10.1016/j.envsoft.2016.02.008

Poirier-Pocovi, M., Bailey, B.N., 2020. Sensitivity analysis of four crop water stress indices to ambient environmental conditions and stomatal conductance. *Sci. Hortic.* 259, *in press*. https://doi.org/10.1016/j.scienta.2019.108825

Struthers, R., Ivanova, A., Tits, L., Swennen, R., Coppin, P., 2015. Thermal infrared imaging of the temporal variability in stomatal conductance for fruit trees. *Int. J. Appl. Earth Obs.* 39: 9-17. https://doi.org/10.1016/j.jag.2015.02.006

Willmott, C.J., 1982. Some comments on the evaluation of modelperformance. *Bull. Am. Meteorol. Soc.* 63,1309–1313. https://doi.org/10.1093/treephys/tpq087

Woods, H.A., Saudreau, M., Pincebourde, S., 2018. Structure is more important than physiology for estimating intracanopy distributions of leaf temperatures. *Ecol. Evol.* 8, 5206-5218. https://doi.org/10.1002/ece3.4046